

1 **Answers to editor/reviewer comments BGD:**

2 We are thankful for made corrections, suggestions and really constructive comments of both  
3 reviewers as well as the editor. We hope we were able to address everything which was addressed  
4 by the recent revision.

5  
6 **Editor review (minor revision):**

7 I read your responses to referee's comment and the new version of manuscript, and I am satisfied  
8 by the work done. I would simply ask you to use the relevant terms when you present your C  
9 storage data (as suggested by referee 2): deltaSOC should be used when you refer to change in  
10 SOC stock, and NCS (or NECB) when you refer to ecosystem C sequestration. Indeed, the results  
11 from these two methods might diverge in some ecosystems depending on the importance of  
12 specific fluxes (p.e. C leaching) that must be considered/evaluated.

13 We changed the MS and Fig. 2, Fig. 6 as well as figure/table captions (Fig. 1, Fig. 2, Fig. 5, Fig.  
14 6, Tab. 1) as suggested. Made changes are marked within the marked up version of the MS (dark  
15 green).

16  
17 **List of relevant changes in the MS:**

- 18 - Changes within the MS:
- 19 ○ As suggested,  $\Delta$ SOC is now used when we refer to change in SOC stock, and
  - 20 NCS (or NECB) when we refer to ecosystem C sequestration
  - 21 ○ The telephone number of the corresponding author was refreshed
  - 22 ○ We added a sentence to the Abstract and Introduction regarding the NECB and
  - 23  $\Delta$ SOC relation and its use within this MS

- 24                   ○ We added a sentence to 4.1 addressing the different theoretical concepts behind  
25                   NECB and  $\Delta$ SOC
- 26                   ○ A “leftover” text fragment was deleted from the conclusions
- 27                   ○ We refreshed the reference of Leiber-Sauheitl et al. (now referred to as  
28                   Biogeosciences instead of Biogeosciences Discussion)
- 29       - Changes in Figures and Tables:
- 30                   ○ Tab.1:
- 31                         ▪ NECB instead of  $\Delta$ SOC is used for chamber derived C budgets
- 32                   ○ Fig.2:
- 33                         ▪  $\Delta$ SOC within the figure was changed for NECB
- 34                   ○ Fig.6:
- 35                         ▪ We added  $\Delta$ SOC and NECB in brackets to the figure legend
- 36
- 37
- 38
- 39
- 40
- 41
- 42
- 43
- 44
- 45
- 46
- 47

48 **Detecting small-scale spatial heterogeneity and temporal dynamics of soil organic carbon**  
49 **(SOC) stocks: a comparison between automatic chamber-derived C budgets and repeated**  
50 **soil inventories**

51  
52 Mathias Hoffmann<sup>a,\*</sup>, Nicole Jurisch<sup>b</sup>, Juana Garcia Alba<sup>a</sup>, Elisa Albiac Borraz<sup>a</sup>, Marten Schmidt<sup>b</sup>,  
53 Vytas Huth<sup>b</sup>, Helmut Rogasik<sup>a</sup>, Helene Rieckh<sup>a</sup>, Gernot Verch<sup>c</sup>, Michael Sommer<sup>a, d</sup>, Jürgen  
54 Augustin<sup>b</sup>

55  
56 <sup>a</sup>Institute of Soil Landscape Research, Leibniz Centre for Agricultural Landscape Research  
57 (ZALF), Eberswalder Str. 84, 15374 Müncheberg, Germany

58 <sup>b</sup>Institute of Landscape Biogeochemistry, Leibniz Centre for Agricultural Landscape Research  
59 (ZALF), Eberswalder Str. 84, 15374 Müncheberg, Germany

60 <sup>c</sup>Research Station Dedelow, Leibniz Centre for Agricultural Landscape Research (ZALF),  
61 Eberswalder Str. 84, 15374 Müncheberg, Germany

62 <sup>d</sup>Institute of Earth and Environmental Sciences, University Potsdam, Karl-Liebknecht-Str.24-25,  
63 14476 Potsdam, Germany

64  
65 \*Corresponding author:

66 Mathias Hoffmann  
67 Eberswalder Str. 84, 15374 Müncheberg, Germany

68 E-mail: Mathias.Hoffmann@zalf.de

69 Tel.: +49(0)33432 82 4068

70 Fax: +49(0)33432 82 280

71 **Abstract**

72 Carbon (C) sequestration in soils plays a key role in the global C cycle. It is therefore crucial to  
73 adequately monitor dynamics in soil organic carbon ( $\Delta$ SOC) stocks when aiming to reveal  
74 underlying processes and potential drivers. However, small-scale spatial (10-30 m) and temporal  
75 changes in SOC stocks, particularly pronounced on arable lands, are hard to assess. The main  
76 reasons for this are limitations of the well-established methods. On the one hand, repeated soil  
77 inventories, often used in long-term field trials, reveal spatial patterns and trends in  $\Delta$ SOC but  
78 require a longer observation period and a sufficient number of repetitions. On the other hand, eddy  
79 covariance measurements of C fluxes towards a complete C budget of the soil-plant-atmosphere  
80 system may help to obtain temporal  $\Delta$ SOC patterns but lack small-scale spatial resolution.

81 To overcome these limitations, this study presents a reliable method to detect both short-term  
82 temporal dynamics as well as small-scale spatial differences of  $\Delta$ SOC using measurements of the  
83 net ecosystem carbon balance (NECB) as a proxy. To estimate the NECB, a combination of  
84 automatic chamber (AC) measurements of CO<sub>2</sub> exchange and empirically modeled aboveground  
85 biomass development ( $NPP_{shoot}$ ) were used. To verify our method, results were compared with  
86  $\Delta$ SOC observed by soil resampling.

87 Soil resampling and AC measurements were performed from 2010 to 2014 at a colluvial depression  
88 located in the hummocky ground moraine landscape of NE Germany. The measurement site is  
89 characterized by a variable groundwater level (GWL) and pronounced small-scale spatial  
90 heterogeneity regarding SOC and nitrogen (Nt) stocks. Tendencies and magnitude of  $\Delta$ SOC values  
91 derived by AC-measurements and repeated soil inventories corresponded well. The period of  
92 maximum plant growth was identified as being most important for the development of spatial  
93 differences in annual  $\Delta$ SOC. Hence, we were able to confirm that AC-based C budgets are able to  
94 reveal small-scale spatial differences and short-term temporal dynamics of  $\Delta$ SOC.

95

96 **Keywords**

97 Net ecosystem exchange (NEE), net primary productivity (NPP), biomass modeling, soil

98 resampling

99

## 100 **1. Introduction**

101 Soils are the largest terrestrial reservoirs of organic carbon (SOC), storing two to three times as  
102 much C as the atmosphere and biosphere (Chen et al., 2015; Lal et al., 2004). In the context of  
103 climate change mitigation as well as soil fertility and food security, there has been considerable  
104 interest in the development of SOC, especially in erosion-affected agricultural landscapes (Berhe  
105 and Kleber, 2013; Conant et al., 2011; Doetterl et al., 2016; Stockmann et al., 2015; Van Oost et  
106 al., 2007; Xiong et al., 2016). Detecting the development of soil organic carbon stocks ( $\Delta$ SOC) in  
107 agricultural landscapes needs to consider three major challenges: First, the high small-scale spatial  
108 heterogeneity of SOC (e.g., Conant et al., 2011; Xiong et al., 2016). Erosion and land use change  
109 reinforce natural spatial and temporal variability, especially in hilly landscapes such as hummocky  
110 ground moraines where correlation lengths in soil parameters of 10-30 m are very common.  
111 Second, pronounced short-term temporal dynamics, caused by, e.g., type of cover crop, frequent  
112 crop rotation and soil cultivation practices. Third, the rather small magnitude of  $\Delta$ SOC compared  
113 to total SOC stocks (e.g., Conant et al., 2011; Poeplau et al., 2016).

114 However, information on the development of SOC is an essential precondition to improve the  
115 predictive ability of terrestrial C models (Luo et al., 2014). As a result, sensitive measurement  
116 techniques are required to precisely assess short-term temporal and small-scale (10-30 m) spatial  
117 dynamics in  $\Delta$ SOC (Batjes and van Wesemael, 2015). To date, the assessment of  $\Delta$ SOC is typically  
118 based on two methods, namely (i) destructive, repeated soil inventories through soil resampling  
119 and (ii) non-destructive determination of ecosystem C budgets (NECB) by measurements of  
120 gaseous C exchange, C import and C export (Leifeld et al., 2011; Smith et al., 2010).

121 The first method is usually used during long-term field trials (Batjes and van Wesemael, 2015;  
122 Chen et al., 2015; Schrumpf et al., 2011). Given a sufficient time horizon of 5 to 10 years, the soil  
123 resampling method is generally able to reveal spatial patterns and trends within  $\Delta$ SOC (Batjes and

124 van Wesemael, 2015; Schrumpf et al., 2011). Most repeated soil inventories are designed to study  
125 treatment differences in the long-term. As a result, short-term temporal dynamics in C exchange  
126 remain concealed (Poeplau et al., 2016; Schrumpf et al., 2011). A number of studies tried to  
127 overcome this methodical limitation by increasing (e.g., monthly) the soil sampling frequency  
128 (Culman et al., 2013; Wuest, 2014). This allows for the detection of seasonal patterns of  $\Delta$ SOC but  
129 still mixes temporal and spatial variability of SOC because every new soil sample represents not  
130 only a repetition in time but also in space. Temporal differences observed through repeated soil  
131 sampling are therefore always spatially biased.

132 By contrast, the NECB (Smith et al. 2010) - used as a proxy for temporal dynamics of  $\Delta$ SOC - can  
133 be easily derived through the eddy covariance (EC) technique, representing a common approach to  
134 obtain gaseous C exchange (Alberti et al., 2010; Leifeld et al., 2011; Skinner and Dell, 2015).  
135 However, C fluxes based on EC measurements are integrated over a larger, altering footprint area  
136 (several hectares). As a result, small-scale (< 20 m) spatial differences in NECB and  $\Delta$ SOC are not  
137 detected.

138 Accounting for the above-mentioned methodical limitations, a number of studies investigated  
139 spatial patterns in gaseous C exchange by using manual chamber measurement systems  
140 (Eickenscheidt et al., 2014; Pohl et al., 2015). Compared to EC measurements, these systems are  
141 characterized by a low temporal resolution, where the calculated net ecosystem CO<sub>2</sub> exchange  
142 (NEE) is commonly based on extensive gap filling (Gomez-Casanovas et al., 2013; Savage and  
143 Davidson, 2003) conducted, e.g., using empirical modeling (Hoffmann et al., 2015). Therefore,  
144 management practices and different stages in plant development that are needed to precisely detect  
145 NEE often remain unconsidered (Hoffmann et al., 2015).

146 Compared to mentioned approaches for detecting  $\Delta$ SOC by either repeated soil sampling or  
147 observations of the gaseous C exchange (NECB), automatic chamber (AC) systems combine

148 several advantages. On the one hand flux measurements of the same spatial entity avoid the mixing  
149 of spatial and temporal variability, as done in case of point measurements by repeated soil  
150 inventories. On the other hand, AC measurements combine advantages of EC and manual chamber  
151 systems because they not only increase the temporal resolution compared to manual chambers but  
152 also allow for the detection of small-scale spatial differences and treatment comparisons regarding  
153 the gaseous C exchange (Koskinen et al., 2014).

154 To date hardly any direct comparisons between AC-derived C budgets and soil resampling-based  
155  $\Delta$ SOC values have been reported in the literature. Leifeld et al. (2011) and Verma et al. (2005)  
156 compared the results of repeated soil inventories with EC-based C budgets over 5- and 3-year study  
157 periods, respectively. Even though temporal dynamics in  $\Delta$ SOC were shown e.g. for grazed  
158 pastures and intensively used grasslands (Skinner and Dell 2015; Leifeld et al., 2011), no attempt  
159 was made to additionally detect small-scale differences in  $\Delta$ SOC. In our study, we introduce the  
160 combination of AC measurements and empirically modeled aboveground biomass production  
161 ( $NPP_{shoot}$ ) as a precise method to detect small-scale spatial differences and short-term temporal  
162 dynamics of **NECB and thus**  $\Delta$ SOC. Measurements were performed from 2010 to 2014 under a  
163 *silage maize/winter fodder rye/sorghum-Sudan grass hybrid/alfalfa* crop rotation at an  
164 experimental plot located in the hummocky ground moraine landscape of NE Germany.

165 We hypothesize that the AC-based C budget method is able to detect small-scale spatial and short-  
166 term temporal dynamics of **NECB and thus**  $\Delta$ SOC in an accurate and precise manner. Therefore,  
167 we compare  $\Delta$ SOC values measured by soil resampling with **NECB** values derived through AC-  
168 based C budgets (Fig. 1).

169

## 170 **2. Materials and methods**

### 171 **2.1 Study site and experimental setup**



172 Measurements were performed at the 6-ha experimental field “CarboZALF-D”. The site is located  
173 in a hummocky arable soil landscape within the Uckermark region (NE-Germany; 53°23`N,  
174 13°47`E, ~50-60 m a.s.l.). The temperate climate is characterized by a mean annual [air](#) temperature  
175 of 8.6°C and annual precipitation of 485 mm (1992–2012, ZALF research station, Dedelow).  
176 Typical landscape elements vary from flat summit and depression locations with a gradient of  
177 approximately 2 %, across longer slopes with a medium gradient of approx. 6 %, to short and rather  
178 steep slopes with a gradient of up to 13 %. The study site shows complex soil patterns mainly  
179 influenced by erosion, relief and parent material, e.g., sandy to marly glacial and glaciofluvial  
180 deposits. The soil type inventory of the experimental site consists of non-eroded Albic Luvisols  
181 (Cutanic) at the flat summits, strongly eroded Calcic Luvisols (Cutanic) on the moderate slopes,  
182 extremely eroded Calcaric Regosols on the steep slopes, and a colluvial soil, i.e., Endogleyic  
183 Colluvic Regosols (Eutric), over peat in the depression (IUSS Working Group WRB, 2015).  
184 During June 2010, four automatic chambers and a WXT520 climate station (Vaisala, Vantaa,  
185 Finland) were set up at the depression (Sommer et al., 2016) ([see 2.2.1](#)). The chambers were  
186 arranged along a topographic gradient (upper (A), upper middle (B), lower middle (C), and lower  
187 (D) chamber position; length ~30 m; difference in altitude ~1 m) within in a distance of approx. 5  
188 m of each other (Fig. 2). As part of the CarboZALF project, a manipulation experiment was carried  
189 out at the end of October 2010, i.e., after the vegetation period (Deumlich et al., 2017). Topsoil  
190 material from a neighboring hillslope was incorporated into the upper soil layer of the depression  
191 (Ap horizon). The amount of translocated soil was equivalent to tillage erosion of a decennial time  
192 horizon (Sommer et al., 2016). The change in SOC for each chamber was monitored by three  
193 topsoil inventories, carried out (I) prior to soil manipulation during April 2009, (II) after soil  
194 manipulation during April 2011, and (III) during December 2014.  $\Delta$ SOC derived through soil

195 resampling and AC-based C budgets (NECB), was compared for the period between April 2011  
196 and December 2014 (Fig. 1).

197 Records of meteorological conditions (1 min frequency) include measurements of air temperature  
198 at 20 cm and 200 cm height, PAR (inside and outside the chamber), air humidity, precipitation, air  
199 pressure, wind speed and direction. Soil temperatures at depths of 2 cm, 5 cm, 10 cm and 50 cm  
200 were recorded using thermocouples, installed next to the climate station (107, Campbell Scientific,  
201 UT, USA).

202 The groundwater level (GWL) was measured using tensiometers assuming hydrostatic equilibrium.  
203 The tensiometers were installed at a soil depth of 160 cm, at soil profile locations in the upper and  
204 lower end of the transect. The average GWL of both profiles was used for further data analysis.  
205 Data gaps < 2 days were filled using simple linear interpolation. Larger gaps in GWL did not occur.  
206 The measurement site was cultivated with five different crops during the study period, following a  
207 practice-orientated and erosion-expedited farming procedure. The crop rotation was silage maize  
208 (*Zea mays*) - winter fodder rye (*Secale cereale*) - sorghum-Sudan grass hybrid (*Sorghum bicolor* x  
209 *sudanese*) - winter triticale (*Triticosecale*) - alfalfa (*Medicago sativa*). Cultivation and fertilization  
210 details are presented in Tab. A.1. Aboveground biomass (NPP<sub>shoot</sub>) development was monitored  
211 using up to four biomass sampling campaigns during the growing season, covering the main growth  
212 stages. Additional measurements of leaf area index (LAI) started in 2013. Collected biomass  
213 samples were chopped and dried to a constant weight (48 h at 105°C). The C, N, K and P contents  
214 were determined using elementary analysis (C, N: TruSpec CNS analyzer, LECO Ltd.,  
215 Mönchengladbach, Germany) and Kjehldahl digestion (P, K; AT200, BeckmanCoulter (Olympus),  
216 Krefeld, Germany and AAS-iCE3300, ThermoFisher-SCIENTIFIC GmbH, Darmstadt, Germany).  
217 To assess the potential impact of chamber placement on plant growth, chemical analyses were

218 carried out for the final harvests of each chamber and compared to biomass samples collected next  
219 to each chamber.

220

## 221 **2.2 C budget method**

### 222 **2.2.1 Automatic chamber system**

223 Automatic flow-through non-steady-state (FT-NSS) chamber measurements (Livingston and  
224 Hutchinson, 1995) of CO<sub>2</sub> exchange were conducted from January 2010 until December 2014. The  
225 AC system consists of 4 identical, rectangular, transparent polycarbonate chambers (thickness of 2  
226 mm; light transmission ~70 %). Each chamber has a height of 2.5 m and covers a surface area of  
227 2.25 m<sup>2</sup> (volume: 5.625 m<sup>3</sup>). To adapt for plant height (alfalfa), the chamber volume was reduced  
228 to 3.375 m<sup>3</sup> in autumn 2013. Airtight closure during measurements was ensured by a rubber belt  
229 that sealed at the bottom of each chamber. A 30-cm open-ended tube on the slightly concave top  
230 of the chambers guided rain water into the chamber and additionally assured pressure equalization.  
231 Two small axial fans (5.61 m<sup>3</sup> min<sup>-1</sup>) were used for mixing the chamber headspace. The chambers  
232 were mounted onto steel frames with a height of 6 m and lifted between measurements using  
233 electrical winches at the top. For controlling the AC system and data collection, a CR1000 data  
234 logger was used (Campbell Scientific, UT, USA). The CO<sub>2</sub> concentration changes over time were  
235 measured within each chamber using a carbon dioxide probe (GMP343, Vaisala, Vantaa, Finland)  
236 connected to a vacuum pump (0.001 m<sup>3</sup> min<sup>-1</sup>; DC12/16FK, Fürgut, Tannheim, Germany). All CO<sub>2</sub>  
237 probes were calibrated prior to installation using ± 0.5 % accurate gases containing 0 ppm, 200  
238 ppm 370 ppm, 600 ppm, 1000, ppm and 4000 ppm CO<sub>2</sub>. The operation schedule of the AC system,  
239 decisively influenced by agricultural treatments, is presented in A.2. The chambers closed in  
240 parallel at an hourly frequency, providing one flux measurement per chamber and hour. The  
241 measurement duration was 5-20 minutes, depending on season and time of day. Nighttime

242 measurements usually lasted 10 min during the growing season and 20 min during the non-growing  
243 season (due to lower concentration increments). The length of the daytime measurements was up  
244 to 10 min, depending on low PAR fluctuations (< 20 %). CO<sub>2</sub> concentrations (inside the chamber)  
245 and general environmental conditions, such as PAR (SKP215, Skye, Llandridd Wells, UK) and  
246 air temperatures (107, Campbell Scientific, UT, USA), were recorded inside and outside the  
247 chambers at a 1 min frequency from 2010 to 2012 and a 15 sec frequency from October 2012.

248

### 249 **2.2.2 CO<sub>2</sub> flux calculation and gap filling**

250 An adaptation of the modular R program script, described in detail by Hoffmann et al. (2015), was  
251 used for stepwise data processing. The atmospheric sign convention was used for the components  
252 of gaseous C exchange (ecosystem respiration (R<sub>eco</sub>; sum of autotrophic and heterotrophic  
253 respiration), gross primary production (GPP) and NEE), whereas positive values for **NECB**  
254 indicate a gain and negative values a loss in SOC. Based on records of environmental variables and  
255 CO<sub>2</sub> concentration change within the chamber headspace, CO<sub>2</sub> fluxes were calculated and  
256 parameterized for R<sub>eco</sub> and GPP within an integrative step. Subsequently, R<sub>eco</sub>, GPP, and NEE were  
257 modeled for the entire measurement period using climate station data. Statistical analyses, model  
258 calibration and comprehensive error prediction were provided for all steps of the modeling process.  
259 CO<sub>2</sub> fluxes ( $F$ ,  $\mu\text{mol C m}^{-2} \text{ s}^{-1}$ ) were calculated according to the ideal gas law (Eq. 1).

260

$$261 \quad F = \frac{pV}{RTA} * \frac{\Delta c}{\Delta t} \quad [\text{Eq. 1}]$$

262

263 where  $\Delta c/\Delta t$  is the concentration change over measurement time, A and V denote the basal area  
264 and chamber volume, respectively, and T and p represent the air temperature inside the chamber  
265 (K) and air pressure. Because plants below the chambers accounted for < 0.2 % of the total chamber

266 volume, a static chamber volume was assumed.  $R$  is a constant ( $8.3143 \text{ m}^3 \text{ Pa K}^{-1} \text{ mol}^{-1}$ ). To  
267 calculate  $\Delta c/\Delta t$ , data subsets based on a variable moving window with a minimum length of 4  
268 minutes were used (Hoffmann et al., 2015).  $\Delta c/\Delta t$  was computed by applying a linear regression to  
269 each data subset, relating changes in chamber headspace  $\text{CO}_2$  concentration to measurement time  
270 (Leiber-Sauheitl et al., 2013; Leifeld et al., 2014; Pohl et al., 2015). In the case of the 15-sec  
271 measurement frequency, a death-band of 5 % was applied prior to the moving window algorithm.  
272 Thus, data noise that originated from either turbulence or pressure fluctuation caused by chamber  
273 deployment or from increasing saturation and canopy microclimate effects was excluded  
274 (Davidson et al., 2002; Kutzbach et al., 2007; Langensiepen et al., 2012). Due to the low  
275 measurement frequency, no data points were discarded for records with 1-min measurement  
276 frequency (2010-2012). The resulting  $\text{CO}_2$  fluxes per measurement (based on the moving window  
277 data subsets) were further evaluated according to the following exclusion criteria: (i) range of  
278 within-chamber air temperature not larger than  $\pm 1.5 \text{ K}$  ( $R_{\text{eco}}$  and NEE fluxes) and a PAR deviation  
279 (NEE fluxes only) not larger than  $\pm 20 \%$  of the average to ensure stable environmental conditions  
280 within the chamber throughout the measurement; (ii) significant regression slope ( $p \leq 0.1$ ,  $t$ -test);  
281 and (iii) non-significant tests ( $p > 0.1$ ) for normality (Lillifor's adaption of the Kolmogorov-  
282 Smirnov test), homoscedasticity (Breusch-Pagan test) and linearity of  $\text{CO}_2$  concentration data.  
283 Calculated  $\text{CO}_2$  fluxes that did not meet all exclusion criteria were discarded. In cases where more  
284 than one flux per measurement met all exclusion criteria, the  $\text{CO}_2$  flux with the steepest slope was  
285 chosen.

286 To account for measurement gaps and to obtain cumulative NEE values, empirical models were  
287 derived based on nighttime  $R_{\text{eco}}$  and daytime NEE measurements following Hoffmann et al. (2015).  
288 For  $R_{\text{eco}}$ , temperature-dependent Arrhenius-type models were used and fitted for recorded air as  
289 well as soil temperatures in different depths (Lloyd and Taylor 1994; Eq. 2).

290

$$291 \quad R_{eco} = R_{ref} * e^{E_0 \left( \frac{1}{T_{ref}-T_0} - \frac{1}{T-T_0} \right)} \quad [Eq. 2]$$

292

293 where  $R_{eco}$  is the measured ecosystem respiration rate [ $\mu\text{mol}^{-1} \text{C m}^{-2} \text{s}^{-1}$ ],  $R_{ref}$  is the respiration rate  
294 at the reference temperature (283.15 K;  $T_{ref}$ );  $E_0$  is an activation energy like parameter;  $T_0$  is the  
295 starting temperature constant (227.13 K) and  $T$  is the mean air or soil temperature during the flux  
296 measurement. Out of the four  $R_{eco}$  models (one model for air temperature, soil temperature in 2 cm,  
297 5 cm and 10 cm depth) obtained for nighttime  $R_{eco}$  measurements of a certain period, the model  
298 with the lowest Akaike Information Criterion (AIC) was used.

299 GPP fluxes were derived using a PAR-dependent, rectangular hyperbolic light response function  
300 based on the Michaelis-Menten kinetic (Elsgaard et al., 2012; Hoffmann et al., 2015; Wang et al.,  
301 2013; Eq. 3). Because GPP was not measured directly, GPP fluxes were calculated as the difference  
302 between measured NEE and modeled  $R_{eco}$  fluxes.

303

$$304 \quad GPP = \frac{GP_{max} * \alpha * PAR}{\alpha * PAR + GP_{max}} \quad [Eq. 3]$$

305

306 where  $GPP$  is the calculated gross primary productivity [ $\mu\text{mol}^{-1} \text{CO}_2 \text{m}^{-2} \text{s}^{-1}$ ];  $GP_{max}$  is the  
307 maximum rate of C fixation at infinite PAR [ $\mu\text{mol CO}_2 \text{m}^{-2} \text{s}^{-1}$ ];  $\alpha$  is the light use efficiency [ $\text{mol}$   
308  $\text{CO}_2 \text{mol}^{-1} \text{photons}$ ] and  $PAR$  is the photon flux density (inside the chamber) of the  
309 photosynthetically active radiation [ $\mu\text{mol}^{-1} \text{photons m}^{-2} \text{s}^{-1}$ ]. In cases where the rectangular  
310 hyperbolic light response function did not result in significant parameter estimates, a non-  
311 rectangular hyperbolic light-response function was used (Gilmanov et al. 2007, 2013; Eq. 4).

312

313 
$$GPP = \alpha * PAR + GP_{max} - \sqrt{(\alpha * PAR + GP_{max})^2 - 4 * \alpha * PAR * GP_{max} * \theta}$$
 [Eq. 4]

314

315 where  $\theta$  is the convexity coefficient of the light-response equation (dimensionless).

316 Due to plant growth and season, parameters of derived  $R_{eco}$  and GPP models may vary with time.

317 To account for this, a moving window parameterization was performed, by applying fluxes of a

318 variable time window (2-21 consecutive measurement days) to Eq.2-4. Temporally overlapping

319  $R_{eco}$  and GPP model sets were evaluated and discarded in case of positive (GPP), negative ( $R_{eco}$ )

320 or insignificant parameter estimates. Finally, the model set with the lowest AIC ( $R_{eco}$ ) was used. If

321 no fit or a non-significant fit was achieved, averaged flux rates were applied for  $R_{eco}$  and GPP. The

322 length of the averaging period was thereby selected by choosing the variable moving window with

323 the lowest standard deviation (SD) of measured fluxes. This procedure was repeated until the whole

324 study period was parameterized.

325 Based on continuously monitored temperature and PAR (outside the chamber),  $R_{eco}$ , GPP and NEE

326 were modeled in half-hour steps for the entire study period. Because GPP was parameterized based

327 on PAR records inside but modeled with PAR records outside the chamber, no PAR correction in

328 terms of reduced light transmission was needed. Uncertainty of annual  $CO_2$  exchange was

329 quantified using a comprehensive error prediction algorithm described in detail by Hoffmann et al.

330 (2015).

331

### 332 **2.2.3 Modeling aboveground biomass dynamics**

333 Aboveground biomass development ( $NPP_{shoot}$ ) was predicted using a logistic empirical model (Yin

334 et al., 2003; Zeide, 1993). From 2010 to 2012, modeled  $NPP_{shoot}$  was based on the relationship

335 between sampling date and the C content of harvested dry biomass measured during sampling

336 campaigns (three to four times per year following plant development). For alfalfa in 2013 and 2014,

337  $NPP_{shoot}$  was modeled based on biweekly measurements of LAI because no additional biomass  
338 sampling was performed between the multiple cuts per year. To calculate the C content  
339 corresponding to the measured LAI, the relationship between LAI prior to the chamber harvest and  
340 the C content measured in the chamber harvest of all six alfalfa cuts was used. Daily values of C  
341 stored within  $NPP_{shoot}$  were calculated using derived logistic functions.

342

#### 343 **2.2.4 Calculation of NECB**

344 Annual **NECB** for each chamber was determined as the sum of annual NEE and  $NPP_{shoot}$ ,  
345 representing C removal due to the chamber harvest (Eq. 4; Leifeld et al., 2014). Temporal dynamics  
346 in **NECB** were calculated as the sum of daily NEE and  $NPP_{shoot}$ .

347

$$348 \quad NECB_n = \sum_{i=1}^n [NEE_i + CH_4 + (NPP_{shoot_i} - C_{import}) + \Delta DOC_i + \Delta DIC_i] \quad [Eq. 5]$$

349

350 Several minor components of Eq. 5 were not considered (see also Hernandez-Ramirez et al., 2011).  
351 First, C import ( $C_{import}$ ) due to seeding and fertilization, which was close to zero because the  
352 measurement site was fertilized by a surface application of mineral fertilizer throughout the entire  
353 study period. Second, methane ( $CH_4$ -C) emissions, which were measured manually at the same  
354 experimental field but did not exceed a relevant order of magnitude ( $-0.01 \text{ g C m}^{-2} \text{ y}^{-1}$ ) and were  
355 therefore not included in the **NECB** calculation. Third, lateral C fluxes, originating from dissolved  
356 organic (DOC) and inorganic carbon (DIC) as well as particulate soil organic carbon ( $SOC_p$ ). In  
357 addition to the rather small magnitude of the subsurface lateral C fluxes in soil solution (Rieckh et  
358 al., 2012), it was assumed that their C input equaled C output at the plot scale. Lateral  $SOC_p$   
359 transport along the hillslope was excluded by grassland stripes established between experimental  
360 plots in 2010 (Fig. 1 in Sommer et al., 2016).



361

362 **2.3 Soil resampling method**

363 To obtain  $\Delta$ SOC using the soil resampling method, soil samples were collected three times during  
364 the study period. Initial SOC along the topographic gradient was monitored prior to soil  
365 manipulation during April 2009 at two soil pits, which were sampled by pedogenetic horizons.  
366 After soil manipulation, a 5-m raster sampling of topsoils (Ap horizons) was performed during  
367 April 2011. Each Ap horizon was separated into an upper (0-15 cm) and lower segment (15-25  
368 cm), which were analyzed separately for bulk density, SOC, Nt and coarse fraction (< 2 mm) (data  
369 not shown). From these data, SOC and Nt mass densities were calculated separately for each  
370 segment and finally summed up for the entire Ap-horizon (0-25 cm). The mean SOC and Nt content  
371 for the Ap horizon of each raster point was calculated by dividing SOC or Nt mass densities (0-25  
372 cm) through the fine-earth mass (0-25 cm). In December 2014, composite soil samples of the Ap  
373 horizon were collected. The composite samples consist of samples from four sampling points in a  
374 close proximity around each chamber. Prior to laboratory analysis coarse organic material was  
375 discarded from collected soil samples (Schlichting et al. 1995). Thermogravimetric desiccation at  
376 105°C was performed in the laboratory for all samples to determine bulk densities ( $\text{Mg m}^{-3}$ ). Bulk  
377 soil samples were air dried, gently crushed and sieved (2 mm) to obtain the fine fraction (particle  
378 size < 2 mm). The total carbon and total nitrogen contents were determined by elementary analysis  
379 (TruSpec CNS analyzer, LECO Ltd., Mönchengladbach, Germany) as carbon dioxide via infrared  
380 detection after dry combustion at 1250°C (DIN ISO10694, 1996), in duplicate. As the soil horizons  
381 did not contain carbonates, total carbon was equal to SOC.

382

383 **2.4 Uncertainty prediction and statistical analysis**

384 Uncertainty prediction for **NECB** derived by the C budget method was performed according to  
385 Hoffmann et al. (2015), following the law of error propagation. To test for differences in topsoil  
386 SOC ( $\text{SOC}_{\text{Ap}}$ ) and total nitrogen (Nt) stocks between soil resampling performed after soil  
387 manipulation in 2010 and 2014, a paired *t*-test was applied. Computation of uncertainty prediction  
388 and calculation of statistical analyses were performed using R 3.2.2.

389

### 390 **3. Results**

#### 391 **3.1 C budget method**

##### 392 **3.1.1 NEE and $\text{NPP}_{\text{shoot}}$ dynamics**

393 NEE and its components  $R_{\text{eco}}$  and GPP were characterized by a clear seasonality and diurnal  
394 patterns. Seasonality followed plant growth and management events (e.g., harvest; Fig. 3), Highest  
395  $\text{CO}_2$  uptake was thus observed during the growing season, whereas NEE fluxes during the non-  
396 growing season were significantly lower. Diurnal patterns were more pronounced during the  
397 growing season and less obvious during the non-growing season. In general  $R_{\text{eco}}$  fluxes were higher  
398 during daytime, whereas GPP and NEE, in case of present cover crops, were lower or even  
399 negative, representing a C uptake during daytime by the plant-soil system. Annual NEE was crop  
400 dependent, ranging from  $-1600 \text{ g C m}^{-2} \text{ y}^{-1}$  to  $-288 \text{ g C m}^{-2} \text{ y}^{-1}$ . Highest annual uptakes were  
401 observed for maize and sorghum during 2011 and 2012, whereas alfalfa cultivation showed lower  
402 annual NEE (Tab. 1). From 2010 to 2012, annual NEE followed the topographic gradient, with  
403 higher NEE in the direction of the depression and lower NEE away from the depression. These  
404 small-scale spatial differences in gaseous C exchange changed with alfalfa cultivation. As a result,  
405 only minor differences between the chamber positions were observed, showing no clear trend or  
406 tendency (Tab. 1).

407 C in living biomass (due to biomass sampling campaigns and LAI measurements) and C removals  
408 due to harvest were in general well reflected by modeled  $\text{NPP}_{\text{shoot}}$  (Fig. 4). Annual C removal due  
409 to harvest was clearly crop dependent, with highest  $\text{NPP}_{\text{shoot}}$  for maize and sorghum ranging from  
410  $420 \text{ g C m}^{-2}$  to  $1238 \text{ g C m}^{-2}$ , and lower values in the case of winter fodder rye and alfalfa. Similar  
411 to NEE from 2010 to 2012, annual sums of  $\text{NPP}_{\text{shoot}}$  followed the topographic gradient, with lower  
412 values close to the depression (Tab. 1). Again, lower differences in annual  $\text{NPP}_{\text{shoot}}$  between the  
413 chambers and no spatial trends were found for alfalfa in 2013 and 2014.

414

### 415 **3.1.2 NECB dynamics**

416 Temporal and spatial dynamics of continuously cumulated daily **NECB** values during the four years  
417 after soil manipulation are shown in Fig. 5. Differences in **NECB** were in general less pronounced  
418 during the non-growing season compared to the growing season. During the non-growing season,  
419 differences were mainly driven by differences in  $R_{\text{eco}}$  rather than GPP or  $\text{NPP}_{\text{shoot}}$ . This changed at  
420 the beginning of the growing season, when **NECB** responded to changes in cumulative NEE and  
421  $\text{NPP}_{\text{shoot}}$ . Hence, up to 79 % of the standard deviation of estimated annual **NECB** developed during  
422 the period of maximum plant growth. Except for the lower middle chamber position, alfalfa seemed  
423 to counterbalance spatial differences in **NECB** that developed during previous years (Fig. 5).

424 Annual **NECB** values derived by the C budget method are presented in Tab. 1. Theron based  
425 highest annual SOC gains were obtained in 2012 for winter fodder rye and sorghum-Sudan grass,  
426 reaching an average of  $474 \text{ g C m}^{-2} \text{ y}^{-1}$ . In contrast, maize cultivation during 2011 was characterized  
427 by C losses between  $59 \text{ g C m}^{-2} \text{ y}^{-1}$  and  $169 \text{ g C m}^{-2} \text{ y}^{-1}$ . However, prior to soil manipulation, maize  
428 showed an average SOC gain of  $102 \text{ g C m}^{-2} \text{ y}^{-1}$ .

429

### 430 **3.2 Soil resampling method**

431 As a result of soil translocation in 2010, initially measured SOC<sub>Ap</sub> stocks increased by an average  
432 of 780 g C m<sup>-2</sup>. However, due to the lower C content of the translocated topsoil material (0.76 %),  
433 the SOC<sub>Ap</sub> content of the measurement site dropped by 10 - 14 % after soil manipulation (Tab. 1).  
434 Significant differences (paired *t*-test; *t* = -2.48, *p* < 0.09), which showed an increase in SOC<sub>Ap</sub> of  
435 up to 11 %, were found between SOC<sub>Ap</sub> stocks measured in 2010 and 2014. Three out of the four  
436 chamber positions showed a C gain during the 4 measurement years following soil manipulation.  
437 C gains were similar for the upper and lower chamber positions, but lower for the upper middle  
438 position. No change in SOC was obtained in the case of the lower middle (Fig. 5; Fig. 6) chamber  
439 position.

440

### 441 **3.3 Method comparison**

442 Average annual  $\Delta$ SOC and NECB values for the soil resampling and C budget method,  
443 respectively, are shown in Fig. 6.  $\Delta$ SOC and NECB showed a good overall agreement, with similar  
444 tendencies and magnitudes (Fig. 6). Irrespective of the applied method, significant differences were  
445 found between SOC stocks measured directly after soil manipulation in 2010 and SOC stocks  
446 measured in 2014. Following soil manipulation, both methods revealed similar tendencies in site  
447 and chamber-specific changes in SOC (Fig. 6). Both methods indicated a clear C gain for three out  
448 of the four chamber positions. C gains derived by the C budget method were similar for the upper,  
449 upper middle and lower chamber positions. By contrast, C gains derived by the soil resampling  
450 method were slightly but not significantly lower (paired *t*-test; *t* = -1.23, *p* > 0.30). This was most  
451 pronounced for the upper middle chamber position. No change in SOC and only a minor gain in C  
452 was observed for the lower middle chamber position according to both methods. Differences  
453 between chamber positions indicate the presence of small-scale spatial  $\Delta$ SOC dynamics typical of  
454 soils.

455

## 456 **4. Discussion**

### 457 **4.1 Accuracy and precision of applied methods**

458 Despite the similar magnitude and tendencies of the observed NECB and  $\Delta$ SOC values, both  
459 methods were subject to numerous sources of uncertainty, representing the different concepts they  
460 are based on (see introduction). These errors affect the accuracy and precision of observed NECB  
461 and  $\Delta$ SOC values differently, which might help to explain differences between the soil resampling  
462 and the C budget method.

463 The soil resampling method is characterized by high measurement precision, which allows for the  
464 detection of relatively small changes in SOC. Related uncertainty in derived spatial and temporal  
465  $\Delta$ SOC dynamics is therefore mainly attributed to the measurement accuracy, affected by sampling  
466 strategy and design (Batjes and van Wesemael, 2015; De Gruijter et al., 2006). This includes (i)  
467 the spatial distribution of collected samples, (ii) the sampling frequency, (iii) the sampling depth  
468 and (iv) whether different components of soil organic matter (SOM) are excluded prior to analyses.  
469 The first aspect determines the capability to detect the inherent spatial differences in SOC stocks.  
470 This allows the conclusion that point measurements do not necessarily represent AC  
471 measurements, which integrate over the spatial variability within their basal area. The second  
472 aspect defines the temporal resolution, even though the soil resampling method is not able to  
473 perfectly separate spatial from temporal variability because repeated soil samples are biased by  
474 inherent spatial variability of the measurement site. The third aspect sets the vertical system  
475 boundary, which is often limited because only topsoil horizons are sampled within a number of soil  
476 monitoring networks (Van Wesemael et al., 2011) and repeated soil inventories (Leifeld et al.,  
477 2011). Similarly, the fourth aspect defines which components of SOM are specifically analyzed.

478 Usually, coarse organic material is discarded prior to analysis (Schlichting et al., 1995) and  
479 therefore, total SOC is not assessed (e.g., roots, harvest residues, etc.).

480 In comparison, the C budget method considers any type of organic material present in soil by  
481 integrating over the total soil depth. As a result, both methods have a different validity range and  
482 area, which makes direct quantitative comparison more difficult. This may explain the higher  
483 uptake reported for three out of four chamber positions in the case of the C budget method.

484 In contrast to the soil resampling method, we postulate a higher accuracy and a lower precision in  
485 the case of the AC-based C budget method. The reasons for this include a number of potential  
486 errors affecting especially the measurement precision of the AC system, whereas over a constant  
487 area and maximum soil depth, integrated AC measurements increase measurement accuracy. First,  
488 it is currently not clear whether microclimatological and ecophysiological disturbances due to  
489 chamber deployment, such as the alteration of temperature, humidity, pressure, radiation, and gas  
490 concentration, may result in biased C flux rate estimates (Juszczak et al., 2013; Kutzbach et al.,  
491 2007; Lai et al., 2012; Langensiepen et al., 2012). Second, uncertainties related to performed flux  
492 separation and gap-filling procedures may influence the obtained annual gaseous C exchange  
493 (Gomez-Casanovas et al., 2013; Görres et al., 2014; Moffat et al., 2007; Reichstein et al., 2005).

494 Although continuous operation of the AC system should allow for direct derivation of C budgets  
495 from measured CO<sub>2</sub> exchange and annual yields, in practice, data gaps always occur. To fill the  
496 measurement gaps, temperature- and PAR-dependent models are derived and used to calculate R<sub>eco</sub>  
497 and GPP, respectively (Hoffmann et al. 2015). Due to the transparent chambers used, modeled R<sub>eco</sub>  
498 is solely based on nighttime measurements. Hence, systematic differences between nighttime and  
499 daytime R<sub>eco</sub> will yield an over- or underestimation of modeled R<sub>eco</sub>. Because modeled R<sub>eco</sub> is used  
500 to calculate GPP fluxes, GPP will be affected in a similar manner. However, the systematic over-  
501 or underestimation of fluxes in both directions may counterbalance the computed NEE, and

502 estimated C budgets may be unaffected. Third, the development of  $NPP_{shoot}$  underneath the  
503 chamber might be influenced by the permanently installed AC system. Fourth, several minor  
504 components such as leaching losses of dissolved inorganic and organic carbon (DIC and DOC), C  
505 transport via runoff and atmospheric C deposition were not considered within the applied budgeting  
506 approach (see also 2.7).

507 Despite the uncertainties mentioned above, error estimates for annual NEE in this study are within  
508 the range of errors presented for annual NEE estimates derived from EC measurements (30 to 50  
509  $g\ C\ m^{-2}\ y^{-1}$ ) (e.g., Baldocchi, 2003; Dobermann et al., 2006; Hollinger et al., 2005) and below the  
510 minimum detectable difference (MDD) reported for most repeated soil inventories (e.g., Batjes and  
511 Van Wesemael, 2015; Knebl et al., 2015; Necpálová et al., 2014; Saby et al., 2008; Schrumpf et  
512 al., 2011; VandenBygaart, 2006).

513

#### 514 **4.2 Plausibility of observed $\Delta SOC$**

515 Both the soil resampling and the C budget method showed C gains during the four years following  
516 soil manipulation. A number of authors calculated additional C sequestration due to soil erosion  
517 (Berhe et al., 2007; Dymond, 2010; VandenBygaart et al., 2015; Yoo et al., 2005), which was  
518 explained by the burial of replaced C at depositional sites and dynamic replacement at eroded sites  
519 (e.g., Doetterl et al., 2016). This is in accordance with erosion-induced C sequestration postulated  
520 by, e.g., Berhe and Kleber (2013) and Van Oost et al. (2007). In addition, observed C sequestration  
521 could also be a result of the manipulation-induced saturation deficit in SOC. By adding topsoil  
522 material from an eroded unsaturated hill slope soil, the capacity and efficiency to sequester C was  
523 theoretically increased (Stewart et al., 2007). Hence, additional C was stored at the measurement  
524 site. This might be due to physicochemical processes, such as physical protection in macro- and

525 micro aggregates (Six et al., 2002) or chemical stabilization by clay and iron minerals (Kleber et  
526 al., 2015).

527 Irrespective of the similar C gain observed by both methods, crop-dependent differences in **NECB**  
528 **and thus**  $\Delta$ SOC were only revealed by the C budget method. The reason is the higher temporal  
529 resolution of AC-derived C budgets, displaying daily C losses and gains. Observed crop-dependent  
530 differences in **NECB** are in accordance with, e.g., Kutsch et al. (2010), Jans et al. (2010), Hollinger  
531 et al. (2005) and Verma et al. (2005), who reported comparable EC-derived C balances for inter  
532 alia, maize, sorghum and alfalfa.

533 In 2012, substantial positive annual **NECB** values were observed. Due to low precipitation during  
534 May and June, germination and plant growth of sorghum-Sudan grass was delayed (Fig. 4). As a  
535 result, the reproductive phenological stage was drastically shortened. This reduced C losses prior  
536 to harvest due to higher  $R_{\text{eco}}:\text{GPP}$  ratios (Wagle et al., 2015). In addition, the presence of cover  
537 crops during spring and autumn could have increased SOC, as reported by Lal et al. (2004),  
538 Ghimire et al. (2014) and Sainju et al. (2002). No additional C sequestration was observed for  
539 alfalfa in 2013 and 2014 or for the lower middle chamber position, which acted neither as a net C  
540 source nor sink (Tab. 1; Fig. 5). This opposes the assumption of increased C sequestration by  
541 perennial grasses (Paustian et al., 1997) or perennial crops (Zan et al., 2001). However, NEE  
542 estimates of alfalfa were within the range of -100 to -400 g C m<sup>-2</sup>, which is typical for forage crops  
543 (*Lolium*, alfalfa, etc.) in different agro-ecosystems (Bolinder et al., 2012; Byrne et al., 2005;  
544 Gilmanov et al., 2013; Zan et al., 2001). In addition, Alberti et al. (2010) reported a soil C loss of  
545 > 170 g C m<sup>-2</sup> after crop conversion from continuous maize to alfalfa, concluding that no effective  
546 C sequestration occurs in the short-term.



547 Regardless of the crop type, the AC-derived dynamic **NECB** values showed that up to 79 % of the  
548 standard deviation of estimated annual **NECB** occurred during the growing season and the main  
549 plant growth period from the beginning of July to the end of September.

550

## 551 **5. Conclusions**

552 We confirmed that AC-based C budgets are in principle able to detect small-scale spatial  
553 differences in **NECB** and might be thus used to detect spatial heterogeneity of  $\Delta$ SOC similar to the  
554 soil resampling method. However, compared to soil resampling, AC-based C budgets also reveal  
555 short-term temporal dynamics (Fig. 5). In addition, AC-based **NECB** values corresponded well  
556 with tendencies and magnitude of  $\Delta$ SOC values observed by the repeated soil inventory. The period  
557 of maximum plant growth was identified as being most important for the development of spatial  
558 differences in annual **NECB**. For upscaling purposes of the presented results, further environmental  
559 drivers, processes and mechanisms determining C allocation in space and time within the plant-  
560 soil system need to be identified. This type of an approach will be pursued in future within the  
561 CarboZALF experimental setup (Sommer et al., 2016; Wehrhan et al., 2016). Moreover, the AC-  
562 based C budget method opens new prospects for clarifying unanswered questions, such as the  
563 influence of plant development or erosion on **NECB** and thereon based estimates of  $\Delta$ SOC.

564

## 565 **Acknowledgments**

566 This work was supported by the Brandenburg Ministry of Infrastructure and Agriculture (MIL),  
567 who financed the land purchase, the Federal Agency for Renewable Resources (FNR), who co-  
568 financed the AC system, and the interdisciplinary research project CarboZALF. The authors want  
569 to express their special thanks to Mr. Peter Rakowski for excellent operational and technical

570 maintenance during the study period as well as to the employees of the ZALF research station,  
571 Dedelow, for establishing and maintaining the CarboZALF-D field trial.

572

## 573 **References**

574 Alberti, G., Delle Vedove, G.D., Zuliani, M., Peressotti, A., Castaldi, S., Zerbi, G., 2010. Changes  
575 in CO<sub>2</sub> emissions after crop conversion from continuous maize to alfalfa. *Agric. Ecosyst.*  
576 *Environ.* 136, 139-147.

577 Baldocchi, D.D., 2003. Assessing the eddy covariance technique for evaluating carbon dioxide  
578 exchange rates of ecosystems: past, present and future. *Glob. Change Biol.* 9, 479-492.

579 Batjes, N.H., van Wesemael, B., 2015. Measuring and monitoring soil carbon, in: Banwart, S. A.,  
580 Noellemeyer, E., Milne, E. (Eds.), *Soil Carbon: Science, Management and Policy for*  
581 *Multiple Benefits*. SCOPE Series 71. CABI, Wallingford, UK, pp. 188-201.

582 Berhe, A.A., Harte, J., Harden, J.W., Torn, M.S., 2007. The significance of the erosion-induced  
583 terrestrial carbon sink. *BioScience* 57, 337-346.

584 Berhe, A.A., Kleber, M., 2013. Erosion, deposition, and the persistence of soil organic matter:  
585 mechanistic consideration and problems with terminology. *Earth Surf. Processes*  
586 *Landforms* 38, 908-912.

587 Bolinder, M.A., Kätterer, T., Andrén, O., Parent, L.E., 2012. Estimating carbon inputs to soil in  
588 forage-based crop rotations and modeling the effects on soil carbon dynamics in a Swedish  
589 long-term field experiment. *Can. J. Soil. Sci.* 92, 821-833.

590 Byrne, K.A., Kiely, G., Leahy, P., 2005. CO<sub>2</sub> fluxes in adjacent new and permanent temperate  
591 grasslands. *Agric. For. Meteorol.* 135, 82-92.

592 Chen, L., Smith, P., Yang, Y., 2015. How has soil carbon stock changed over recent decades? *Glob.*  
593 *Change Biol.* 21, 3197-3199.

594 Conant, R.T., Ogle, S.M., Paul, E.A., Paustian, K., 2011. Measuring and monitoring soil organic  
595 carbon stocks in agricultural lands for climate mitigation. *Front. Ecol. Environ.* 9, 169-173.

596 Culman, S.W., Snapp, S.S., Green, J.M., Gentry, L.E., 2013. Short- and long-term labile soil carbon  
597 and nitrogen dynamics reflect management and predict corn agronomic performance.  
598 *Agron. J.* 105, 493-502.

599 Davidson, E. A., Savage, K., Verchot, L. V., Navarro, R., 2002. Minimizing artifacts and biases in  
600 chamber-based measurements of soil respiration. *Agric. For. Meteorol.* 113, 21-37.

601 De Gruijter, J.J., Brus, D.J., Bierkens, M.F.P., Knotters, M., 2006. *Sampling for Natural Resource*  
602 *Monitoring.* Springer Verlag, Berlin.

603 Deumlich, D., Rogasik, H., Hierold, W., Onasch, I., Völker, L., Sommer, M., 2017 (in print). The  
604 CarboZALF-D manipulation experiment – experimental design and SOC patterns. *Int. j.*  
605 *environ. agric. res.* 3, 40-50.

606 Dobermann, A.R., Walters, D.T., Baker, J.M., 2006. Comment on “Carbon budget of mature no-  
607 till ecosystem in north central region of the United States.” *Agric. For. Meteorol.* 136, 83-  
608 84.

609 Doetterl, S., Berhe, A.A., Nadeu, E., Wang, Z., Sommer, M., Fiener, P., 2016. Erosion, deposition  
610 and soil carbon: a review of process-level controls, experimental tools and models to  
611 address C cycling in dynamic landscapes. *Earth Sci. Rev.* 154, 102-122.

612 Dymond, J.R., 2010. Soil erosion in New Zealand is a net sink of CO<sub>2</sub>. *Earth Surf. Processes*  
613 *Landforms* 35, 1763-1772. doi:10.1002/esp.2014.

614 Eickenscheidt, T., Freibauer, A., Heinichen, J., Augustin, J., Drösler, M., 2014. Short-term effects  
615 of biogas digestate and cattle slurry application on greenhouse gas emissions affected by N

616 availability from grasslands on drained fen peatlands and associated organic soils.  
617 Biogeosciences 11, 6187-6207.

618 Elsgaard, L., Görres, C., Hoffmann, C.C., Blicher-Mathiesen, G., Schelde, K., Petersen, S.O., 2012.  
619 Net ecosystem exchange of CO<sub>2</sub> and carbon balance for eight temperate organic soils under  
620 agricultural management. Agric. Ecosyst. Environ. 162, 52-67.

621 Foken, T., 2008. Micrometeorology. Springer Verlag, Berlin.

622 Ghimire, R., Norton, J.B., Pendall, E., 2014. Alfalfa-grass biomass, soil organic carbon, and total  
623 nitrogen under different management approaches in an irrigated agroecosystem. Plant Soil  
624 374, 173-184.

625 Gilmanov, T.G., Soussana, J.F., Aires, L., Allard, V., Ammann, C., Balzarolo, M., Barcza, Z.,  
626 Bernhofer, C., Campbell, C.L., Cernusca, A., Cescatti, A., Clifton-Brown, J., Dirks,  
627 B.O.M., Dore, S., Eugster, W., Fuhrer, J., Gimeno, C., Gruenwald, T., Haszpra, L., Hensen,  
628 A., Ibrom, A., Jacobs, A.F.G., Jones, M.B., Lanigan, G., Laurila, T., Lohila, A., Manca, G.,  
629 Marcolla, B., Nagy, Z., Pilegaard, K., Pinter, K., Pio, C., Raschi, A., Rogiers, N., Sanz,  
630 M.J., Stefani, P., Sutton, M., Tuba, Z., Valentini, R., Williams, M.L., Wohlfahrt, G., 2007.  
631 Partitioning European grassland net ecosystem CO<sub>2</sub> exchange into gross primary  
632 productivity and ecosystem respiration using light response function analysis. Agric.  
633 Ecosyst. Environ. 121, 93–120.

634 Gilmanov, T.G., Wylie, B.K., Tieszen, L.L., Meyers, T.P., Baron, V.S., Bernacchi, C.J.,  
635 Billesbach, D.P., Burba, G.G., Fischer, M.L., Glenn, A.J., Hanan, N.P., Hatfield, J.L.,  
636 Heuer, M.W., Hollinger, S.E., Howard, D.M., Matamala, R., Prueger, J.H., Tenuta, M.,  
637 Young, D.G., 2013. CO<sub>2</sub> uptake and ecophysiological parameters of the grain crops of  
638 midcontinent North America: estimates from flux tower measurements. Agric. Ecosyst.  
639 Environ. 164, 162–175.

640 Gomez-Casanovas, N., Anderson-Teixeira, K., Zeri, M., Bernacchi, C.J., DeLucia, E.H., 2013. Gap  
641 filling strategies and error in estimating annual soil respiration. *Glob. Change Biol.* 19,  
642 1941-1952.

643 Görres, C.-M., Kutzbach, L., Elsgaard, L., 2014. Comparative modeling of annual CO<sub>2</sub> flux of  
644 temperate peat soils under permanent grassland management. *Agric. Ecosyst. Environ.* 186,  
645 64–76.

646 Hernandez-Ramirez, G., Hatfield, J.L., Parkin, T.B., Sauer, T.J., Prueger, J.H., 2011. Carbon  
647 dioxide fluxes in corn-soybean rotation in the midwestern U.S.: inter- and intra-annual  
648 variations, and biophysical controls. *Agric. For. Meteorol.* 151, 1831-1842.

649 Hoffmann, M., Jurisch, N., Borraz, E.A., Hagemann, U., Drösler, M., Sommer, M., Augustin, J.,  
650 2015. Automated modeling of ecosystem CO<sub>2</sub> fluxes based on periodic closed chamber  
651 measurements: a standardized conceptual and practical approach. *Agric. For. Meteorol.*  
652 200, 30-45.

653 Hollinger, S.E., Bernacchi, C.J., Meyers, T.P., 2005. Carbon budget of mature no-till ecosystem in  
654 north central region of the United States. *Agric. For. Meteorol.* 130, 59-69.

655 IUSS Working Group WRB, 2015. World reference base for soil resources 2014. International soil  
656 classification system for naming soils and creating legends for soil maps. Update 2015.  
657 World Soil Resources Reports No. 106. FAO, Rome.

658 Jans, W.W.P., Jacobs, C.M.J., Kruijt, B., Elbers, J.A., Barendse, S., Moors, E.J., 2010. Carbon  
659 exchange of a maize (*Zea mays* L.) crop: influence of phenology. *Agric. Ecosyst. Environ.*  
660 139, 316-324.

661 Juszczak, R., Humphreys, E., Acosta, M., Michalak-Galczewska, M., Kayzer, D., Olejnik, J., 2013.  
662 Ecosystem respiration in a heterogeneous temperate peatland and its sensitivity to peat  
663 temperature and water table depth. *Plant Soil* 366, 505-520.

664 Kleber, M., Eusterhues, K., Keiluweit, M., Mikutta, C., Mikutta, R., Nico, P. S., 2015. Chapter one  
665 – Mineral-Organic associations: Formation, Properties, and relevance in soil environments.  
666 Adv. Agro. 130, 1-140.

667 Knebl, L., Leithold, G., Brock, C., 2015. Improving minimum detectable differences in the  
668 assessment of soil organic matter change in short-term field experiments. J. Plant Nutr. Soil  
669 Sci. 178, 35-42.

670 Koskinen, M., Minkkinen, K., Ojanen, P., Kämäräinen, M., Laurila, T., Lohila, A., 2014.  
671 Measurements of CO<sub>2</sub> exchange with an automated chamber system throughout the year:  
672 challenges in measuring night-time respiration on porous peat soil. Biogeosciences 11, 347-  
673 363.

674 Kutsch, W.L., Aubinet, M., Buchmann, N., Smith, P., Osborne, B., Eugster, W., Wattenbach, M.,  
675 Schruppf, M., Schulze, E.D., Tomelleri, E., Ceschia, E., Bernhofer, C., Béziat, P., Carrara,  
676 A., Di Tommasi, P., Grünwald, T., Jones, M., Magliulo, V., Marloie, O., Moureaux, C.,  
677 Oliosio, A., Sanz, M.J., Saunders, M., Søgaard, H., Ziegler, W., 2010. The net biome  
678 production of full crop rotations in Europe. Agric. Ecosyst. Environ. 139, 336-345.

679 Kutzbach, L., Schneider, J., Sachs, T., Giebels, M., Nykänen, H., Shurpali, N.J., Martikainen, P.J.,  
680 Alm, J., Wilmking, M., 2007. CO<sub>2</sub> flux determination by closed-chamber methods can be  
681 seriously biased by inappropriate application of linear regression. Biogeosciences 4, 1005-  
682 1025.

683 Lai, D.Y.F., Roulet, N.T., Humphreys, E.R., Moore, T.R., Dalva, M., 2012. The effect of  
684 atmospheric turbulence and chamber deployment period on autochamber CO<sub>2</sub> and CH<sub>4</sub> flux  
685 measurements in an ombrotrophic peatland. Biogeosciences 9, 3305-3322.

686 Lal, R., Griffin, M., Apt, J., Lave, L., Morgan, G., M., 2004. Managing Soil carbon. Science 304,  
687 393.

688 Langensiepen, M., Kupisch, M., van Wijk, M.T., Ewert, F., 2012. Analyzing transient closed  
689 chamber effects on canopy gas exchange for flux calculation timing. *Agric. For. Meteorol.*  
690 164, 61-70.

691 Leiber-Sauheitl, K., Fuß, R., Voigt, C., Freibauer, A., 2013. High greenhouse gas fluxes from  
692 grassland on histic gleysol along soil C and drainage grasslands. *Biogeosciences*. 11, 749-  
693 761.

694 Leifeld, J., Ammann, C., Neftel, A., Fuhrer, J., 2011. A comparison of repeated soil inventory and  
695 carbon flux budget to detect soil carbon stock changes after conversion from cropland to  
696 grasslands. *Glob. Change Biol.* 17, 3366-3375.

697 Leifeld, J., Bader, C., Borraz, E., Hoffmann, M., Giebels, M., Sommer, M., Augustin, J., 2014. Are  
698 C-loss rates from drained peatlands constant over time? The additive value of soil profile  
699 based and flux budget approach. *Biogeosci. Discuss.* 11, 12341-12373.

700 Livingston, G.P., Hutchinson, G.L., 1995. Enclosure-based measurement of trace gas exchange:  
701 applications and sources of error, in: Matson, P.A., Harris, R.C. (Eds.), *Methods in Ecology.*  
702 *Biogenic Trace Gases: Measuring Emissions from Soil and Water.* Blackwell Science,  
703 Oxford, UK, pp. 14–51.

704 Lloyd, J., Taylor, J.A., 1994. On the temperature dependence of soil respiration. *Funct. Ecol.* 8,  
705 315-323.

706 Luo, Y., Ahlström, A., Allison, S.D., Batjes, N.H., Brovkin, V., Carvalhais, N., Chappell, A., Ciais,  
707 P., Davidson, E.A., Finzi, A., Georgiou, K., Guenet, B., Hararuk, O., Harden, J.W., He, Y.,  
708 Hopkins, F., Jiang, L., Koven, C., Jackson, R.B., Jones, C.D., Lara, M.J., Liang, J.,  
709 McGuire, A.D., Parton, W., Peng, C., Randerson, J.T., Salazar, A., Sierra, C.A., Smith,  
710 M.J., Tian, H., Todd-Brown, K.E.O., Torn, M., van Groenigen, k.J., Wang, Y.P., West, t.o.,  
711 Wie, Y., Wieder, W.R., Xia, J., Xu, X., Xu, X., Zhou, T., 2016. Toward more realistic

712 projections of soil carbon dynamics by Earth system models. *Global Biogeochem. Cycles*  
713 30, 40-56.

714 Moffat, A.M., Papale D., Reichstein M., Hollinger, D.Y., Richardson, A.D., Barr, A.G., Beckstein,  
715 C., Braswell, B.H., Churkina, G., Desai, A.R., Falge, E., Gove, J.H., Heimann, M., Hui, D.,  
716 Jarvis, A.J., Kattge, J., Noormets, A., Stauch, V.J., 2007. Comprehensive comparison of  
717 gap-filling techniques for eddy covariance net carbon fluxes. *Agric. For. Meteorol.* 147,  
718 209–232.

719 Necpálová, M., Anex Jr., R.P., Kravchenko, A.N., Abendroth, L.J., Del Grosso, S.J., Dick, W.A.,  
720 Helmers, M.J., Herzmann, D., Lauer, J.G., Nafziger, E.D., Sawyer, J.E., Scharf, P.C.,  
721 Strock, J.S., Villamil, M.B., 2014. What does it take to detect a change in soil carbon stock?  
722 A regional comparison of minimum detectable difference and experiment duration in the  
723 north central United States. *J. Soils Water Conserv.* 69, 517-531.

724 Paustian, K., Collins, H.P., Paul, E.A., 1997. Management controls on soil carbon, in: Paul, E.A.,  
725 Paustian, K., Elliott, E.T., Cole, C.V. (Eds.), *Soil Organic Matter in Temperate*  
726 *Agroecosystems: Long-Term Experiments in North America*. CRC Press, Boca Raton, FL,  
727 pp. 15-50.

728 Poeplau, C., Bolinder, M.A., Kätterer, T., 2016. Towards an unbiased method for quantifying  
729 treatment effects on soil carbon in long-term experiments considering initial within-field  
730 variation. *Geoderma* 267, 41-47.

731 Pohl, M., Hoffmann, M., Hagemann, U., Giebels, M., Albiac Borraz, E., Sommer, M., Augustin,  
732 J., 2014. Dynamic C and N stocks—key factors controlling the C gas exchange of maize in  
733 a heterogeneous peatland. *Biogeosciences* 11, 2737-2752.

734 Reichstein, M., Falge, E., Baldocchi, D., Papale, D., Aubinet, M., Berbigier, P., Bernhofer, C.,  
735 Buchmann, N., Gilmanov, T., Granier, A., Grünwald, T., Havránková, K., Ilvesniemi, H.,



736 Janous, D., Knohl, A., Laurila, T., Lohila, A., Loustau, D., Metteucci, G., Meyers, T.,  
737 Miglietta, F., Ourcival, J.-M., Pumpanen, J., Rambal, S., Rotenberg, E., Sanz, M.,  
738 Tenhunen, J., Seufert, G., Vaccari, F., Vesala, T., Yakir, D., Valentini, R., 2005. On the  
739 separation of net ecosystem exchange into assimilation and ecosystem respiration: review  
740 and improved algorithm. *Global Change Biol.* 11, 1424–1439.

741 Rieckh, H., Gerke, H.H., Sommer, M., 2012. Hydraulic properties of characteristic horizons  
742 depending on relief position and structure in a hummocky glacial soil landscape. *Soil*  
743 *Tillage Res.* 125, 123-131.

744 Saby, N.P.A., Bellamy, P.H., Morvan, X., Arrouays, D., Jones, R.J.A., Verheijen, F.G.A.,  
745 Kibblewhite, M.G., Verdoodt, A., Üveges, J.B., Freudenschuß, A., Simota, C., 2008. Will  
746 European soil-monitoring networks be able to detect changes in topsoil organic carbon  
747 content? *Glob. Change Biol.* 14, 2432-2442.

748 Sainju, U.M., Singh, B.P., Whitehead, W.F., 2002. Long-term effects of tillage, cover crops, and  
749 nitrogen fertilization on organic carbon and nitrogen concentrations in sandy loam soils in  
750 Georgia, USA. *Soil Tillage Res.* 63, 167-179.

751 Savage, K.E., Davidson, E.A., 2003. A comparison of manual and automated systems for soil CO<sub>2</sub>  
752 flux measurements: trade-offs between spatial and temporal resolution. *J. Exp. Bot.* 54,  
753 891-899.

754 Schlichting, E., Blume, H.P., Stahr, K., *Soils Practical* (in German). Blackwell, Berlin, 1995.

755 Schrumpf, M., Schulze, E. D., Kaiser, K., Schumacher, J., 2011. How accurately can soil organic  
756 carbon stocks and stock changes be quantified by soil inventories? *Biogeosciences* 8, 1193-  
757 1212.

758 Six, J., Conant, R.T., Paul, E.A., Paustian, K., 2002. Stabilization mechanisms of soil organic  
759 matter: implications for C-saturation of soils. *Plant Soil* 241, 155-176.

760 Skinner, R.H., Dell, C.J., 2015. Comparing pasture C sequestration estimates from eddy covariance  
761 and soil cores. *Agric. Ecosyst. Environ.* 199, 52-57.

762 Smith, P., Lanigan, G., Kutsch, W. L., Buchmann, N., Eugster, W., Aubinet, M., Ceschia, E.,  
763 Béziat, P., Yeluripati, J. B., Osborne, B., Moors, E. J., Brut, A., Wattenbach, M., Saunders,  
764 M., Jones, M., 2010. Measurements necessary for assessing the net ecosystem carbon  
765 budget of croplands. *Agric. Ecosyst. Environ.* 139, 302-315.

766 Sommer, M., Augustin, J., Kleber, M., 2016. Feedbacks of soil erosion on SOC patterns and carbon  
767 dynamics in agricultural landscapes – the CarboZALF experiment. *Soil Tillage Res.* 156,  
768 182-184.

769 Stewart, C.E., Paustian, K., Conant, R.T., Plante, A.F., Six, J., 2007. Soil carbon saturation:  
770 concept, evidence and evaluation. *Biogeochemistry* 86, 19-31.

771 Stockmann, U., Padarian, J., McBratney, A., Minasny, B., de Brogniez, D., Montanarella, L., Hong,  
772 Y., S., Rawlins, B.G., Field, D.J., 2015. Global soil organic carbon assessment. *Glob. Food*  
773 *Secur.* 6, 9-16.

774 Van Oost, K., Quine, T.A., Govers, G., De Gryze, S., Six, J., Harden, J.W., Ritchie, J.C., McCarty,  
775 G.W., Heckrath, G., Kosmas, C., Giraldez, J.V., da Silva, J.R., Merckx, R., 2007. The  
776 impact of agricultural soil erosion on the global carbon cycle. *Science* 318, 626-629.

777 Van Wesemael, B., Paustian, K., Andrén, O., Cerri, C.E.P., Dodd, M., Etchevers, J., Goidts, E.,  
778 Grace, P., Kätterer, T., McConkey, B.G., Ogle, S., Pan, G., Siebner, C., 2011. How can soil  
779 monitoring networks be used to improve predictions of organic carbon pool dynamics and  
780 CO<sub>2</sub> fluxes in agricultural soils? *Plant Soil* 338, 247-259.

781 VandenBygaart, A.J., 2006. Monitoring soil organic carbon stock changes in agricultural  
782 landscapes: issues and a proposed approach. *Can. J. Soil Sci.* 86, 451-463.

783 VandenBygaart, A.J., Gregorich, E.G., Helgason, B.L., 2015. Cropland C erosion and burial: is  
784 buried soil organic matter biodegradable? *Geoderma* 239-240, 240-249.

785 Verma, S.B., Dobermann, A., Cassman, K.G., Walters, D.T., Knops, J.M., Arkebauer, T.J., Suyker,  
786 A.E., Burba, G.G., Amos, B., Yang, H., Ginting, D., Hubbard, K.G., Gitelson, A.A.,  
787 Walter-Shea, E.A., 2005. Annual carbon dioxide exchange in irrigated and rainfed maize-  
788 based agroecosystems. *Agric. For. Meteorol.* 131, 77-96.

789 Wagle, P., Kakani, V.G., Huhnke, R.L., 2015. Net ecosystem carbon dioxide exchange of dedicated  
790 bioenergy feedstocks: switchgrass and high biomass sorghum. *Agric. For. Meteorol.* 207,  
791 107-116.

792 Wang, K., Liu, C., Zheng, X., Pihlatie, M., Li, B., Haapanala, S., Vesala, T., Liu, H., Wang, Y.,  
793 Liu, G., Hu, F., 2013. Comparison between eddy covariance and automatic chamber  
794 techniques for measuring net ecosystem exchange of carbon dioxide in cotton and wheat  
795 fields. *Biogeosciences* 10, 6865-6877.

796 Wehrhan, M., Rauneker, P., Sommer, M., 2016. UAV-based estimation of carbon exports from  
797 heterogeneous soil landscapes - a case study from the CarboZALF experimental area.  
798 *Sensors (Basel)* 16, 255.

799 Wuest, S., 2014. Seasonal variation in soil organic carbon. *Soil Sci. Soc. Am. J.* 78, 1442-1447.

800 Xiong, X., Grunwald, S., Corstanje, R., Yu, C., Bliznyuk, N., 2016. Scale-dependent variability of  
801 soil organic carbon coupled to land use and land cover. *Soil Tillage Res.* 160, 101-109.

802 Yin, X., Goudriaan, J., Lantinga, E.A., Vos, J., Spiertz, H.J., 2003. A flexible sigmoid function of  
803 determinate growth. *Ann. Bot.* 91, 361-371.

804 Yoo, K., Amundson, R., Heimsath, A.M., Dietrich, W.E., 2005. Erosion of upland hillslope soil  
805 organic carbon: coupling field measurements with a sediment transport model. *Global*  
806 *Biogeochem. Cycles* 19, 1-17.

807 Zan, C.S., Fyles, J.W., Girouard, P., Samson, R.A., 2001. Carbon sequestration in perennial  
808 bioenergy, annual corn and uncultivated systems in southern Quebec. *Agric. Ecosyst.*  
809 *Environ.* 86, 135-144.

810 Zeide, B., 1993. Analysis of growth equations. *For. Sci.* 39, 594-616.

811

## 812 **List of tables:**

813 **Tab. 1.:** Chamber-specific annual sums of CO<sub>2</sub> exchange ( $R_{eco}$ , GPP, NEE),  $NPP_{shoot}$ , **NECB** and  
814  $\Delta SOC$  ( $\pm$  uncertainty), as well as corresponding environmental variables measured during the study  
815 period from 2010 to 2014.

816 **A.1.:** Management information regarding the study period from 2010 to 2014. Gray shaded rows  
817 indicate coverage by chamber measurements.

818

## 819 **List of figures:**

820 **Fig. 1.:** Schematic representation of the study concept **used to detect changes in soil organic carbon**  
821 **stock ( $\Delta SOC$ )**. Black stars represent SOC measured by the soil resampling method. Black circles  
822 represent annual **NECB** derived using the C budget method.

823 **Fig. 2.:** Transect of automatic chambers and chamber positions within the depression overlying the  
824 Endogleyic Colluvic Regosol (WRB 2015, left). The black arrow shows the position of the  
825 datalogger and controlling devices, which were placed within a wooden, weather-sheltered house.  
826 The soil profile is shown on the right. Soil horizon-specific SOC (%) and Nt (%) contents are  
827 indicated by solid and dashed vertical white lines, respectively. **Spatial differences in NECB and**  
828 **the basic principle of the C budget method are shown as the scheme within the picture.**

829 **Fig. 3.:** Time series of CO<sub>2</sub> exchange (A-D) for the four chambers of the AC system during the  
830 study period from 2010 to 2014. R<sub>eco</sub> (black), GPP (light gray) and NEE (dark gray) are shown as  
831 daily sums (y-axis). NEE<sub>cum</sub> is presented as a solid line, representing the sum of continuously  
832 accumulated daily NEE values (secondary y-axis). The presented values display cumulative NEE  
833 following soil manipulation to the end of 2014. Note the different scales of the y-axes. The grey  
834 shaded area represents the period prior to soil manipulation. The dashed vertical line indicates the  
835 soil manipulation. Dotted lines represent harvest events.

836 **Fig. 4.:** Time series of modeled aboveground biomass development (NPP<sub>shoot</sub>) (A-D) for the four  
837 chambers of the AC system during the study period from 2010 to 2014. NPP<sub>shoot</sub> is shown as  
838 cumulative values. The presented values display cumulative NPP<sub>shoot</sub> following soil manipulation  
839 to the end of 2014. The biomass model is based on biomass sampling (2010-2012) and biweekly  
840 LAI measurements (2013-2014) during crop growth (grey dots). C removal due to chamber  
841 harvests is shown by black dots. The grey shaded area represents the period prior to soil  
842 manipulation. The dashed vertical line indicates the soil manipulation. Dotted lines represent  
843 harvest events.

844 **Fig. 5.:** Temporal and spatial dynamics in cumulative NECB and ΔSOC throughout the study  
845 period based on (A) the C budget method (measured/modeled; black lines) and (B) the soil  
846 resampling method (linear interpolation; gray lines), **respectively**. The grey shaded area represents  
847 the period prior to soil manipulation. The dashed vertical line indicates the soil manipulation.  
848 Dotted lines represent harvest events. **Temporal dynamics in NECB revealed by the C budget**  
849 **method allow for the identification of periods being most important for changes in SOC. Major**  
850 **spatial deviation occurred during the maximum plant growth period (May to September). The**

851 proportion (%) of these periods with respect to the standard deviation of estimated annual NECB  
852 accounted for up to 79 %.

853 **Fig. 6.:** Average annual  $\Delta$ SOC observed after soil manipulation (April 2011 to December 2014)  
854 by soil resampling and the C budget method for (A) the entire measurement site and (B) single  
855 chamber positions within the measured transect.  $\Delta$ SOC represents the change in carbon storage,  
856 with positive values indicating C sequestration and negative values indicating C losses. Error bars  
857 display estimated uncertainty for the C budget method and the analytical error of  $\pm 5$  % for the soil  
858 resampling method. A performed Wilcoxon rank-sum test showed no significant difference between  
859 NECB and  $\Delta$ SOC values obtained by both methodological approaches for all four chambers (p-  
860 value=0.25).

861 **A.3.:** Time series of recorded environmental conditions throughout the study period from 2010 to  
862 2014. Daily Precipitation and GWL are shown for the upper (solid line) and lower (dashed line)  
863 chamber position in the upper panel (A). The lower panel (B) shows the mean daily air temperature.  
864 The grey shaded area represents the period prior to soil manipulation. The dashed vertical line  
865 indicates the soil manipulation.

866

867

868

869

Tab.1

Year	Crop rotation	Position	R <sub>CO2</sub>	GPP	NEE	NECB*	NPP <sub>above</sub>			SOC to 1 m depth	SOC in Ap horizon	ΔSOC	Nt to 1 m depth	Nt in Ap horizon	Precip.	GWL			
							harvested	modeled	N								P	K	
			(g C m <sup>-2</sup> )				(g C m <sup>-2</sup> )			(g m <sup>-2</sup> )			(Kg m <sup>-2</sup> 1 m <sup>-1</sup> )	(Kg m <sup>-2</sup> 0.3 m <sup>-1</sup> )	(g C m <sup>-2</sup> )	(Kg m <sup>-2</sup> 1 m <sup>-1</sup> )	(Kg m <sup>-2</sup> 0.3 m <sup>-1</sup> )	(mm)	(cm)
2010	maize	A (upper)	1014 ±9	-1845 ±8	-831 ±12	86 ±66	744	745 ±65	28.1	5.0	25.6	11.6	5.1		1.3	0.6	516	135	
		B (upper middle)	987 ±11	-1970 ±8	-983 ±13	251 ±66	727	732 ±64	24.7	4.1	18.0	9.1	4.2		0.9	0.4		103	
		C (lower middle)	1064 ±38	-2000 ±11	-935 ±40	190 ±77	744	745 ±65	25.5	4.2	16.9	9.1	4.2		0.9	0.4		95	
		D (lower)	1110 ±21	-1737 ±10	-627 ±23	-118 ±69	744	745 ±65	25.0	4.2	18.2	12.8	5.0		1.3	0.5		69	
2011	maize	A (upper)	891 ±13	-2022 ±18	-1131 ±22	-149 ±103	1238	1280 ±101	29.5	5.4	30.2	10.5	3.5		1.1	0.4	618	129	
		B (upper middle)	855 ±10	-1894 ±13	-1039 ±16	-169 ±96	1167	1208 ±95	36.4	5.9	32.7	8.7	3.4		0.9	0.4		97	
		C (lower middle)	980 ±14	-2062 ±25	-1082 ±28	-79 ±95	1115	1161 ±91	33.7	5.6	32.9	9.0	3.7		0.9	0.4		87	
		D (lower)	843 ±31	-1730 ±8	-888 ±32	-59 ±80	900	947 ±73	35.0	5.7	31.8	12.2	4.0		1.3	0.4		61	
2012	winter wheat	A (upper)	1058 ±86	-2659 ±12	-1600 ±87	648 ±104	297**/634	952 ±56	36.3	6.3	42.6						585	139	
		B (upper middle)	1075 ±8	-2591 ±11	-1516 ±13	472 ±65	310**/727	1044 ±64	33.3	5.8	37.5							107	
	sorghum	C (lower middle)	1286 ±8	-2617 ±9	-1331 ±12	346 ±60	310**/665	985 ±59	32.7	5.4	35.5							87	
		D (lower)	1044 ±10	-2194 ±9	-1150 ±13	430 ±39	299**/420	720 ±37	33.9	5.8	40.4							61	
2013		A (upper)	1140 ±83	-1583 ±9	-443 ±83	43 ±91	290	400 <sup>ab</sup> ±37	14.0	1.7	11.6						499	154	
		B (upper middle)	1283 ±80	-1819 ±8	-536 ±80	93 ±86	304	443 <sup>b</sup> ±32	14.7	1.8	12.1							122	
		C (lower middle)	1438 ±20	-1726 ±7	-288 ±22	-107 ±36	324	395 ±29	15.6	1.9	12.9							94	
		D (lower)	1587 ±80	-2036 ±8	-448 ±80	6 ±87	329	442 <sup>b</sup> ±34	15.9	2.0	13.2							68	
2014	alfalfa	A (upper)	1161 ±15	-1615 ±7	-455 ±16	-126 ±26	605	581 ±20	29.2	3.6	24.2	10.9	3.9	376	1.2	0.5	591	181	
		B (upper middle)	1443 ±18	-2063 ±7	-619 ±19	52 ±28	635	567 ±20	30.7	3.8	25.4	8.9	3.5	156	0.9	0.4		149	
		C (lower middle)	1683 ±18	-2111 ±6	-428 ±19	-36 ±26	632	535 ±18	30.5	3.8	25.3	9.0	3.7	0	0.9	0.5		121	
		D (lower)	1584 ±12	-2113 ±14	-528 ±19	-52 ±28	587	580 ±21	28.3	3.5	23.5	12.5	4.2	276	1.3	0.4		95	
annual average (2011-2014)		A (upper)	1063 ±49	-1970 ±12	-901 ±52	98 ±43	766	803 ±54	27.3	4.3	27.2			94 ±43				151	
		B (upper middle)	1164 ±29	-2092 ±10	-919 ±32	104 ±37	786	815 ±53	28.8	4.3	26.9			39 ±43				119	
		C (lower middle)	1347 ±15	-2129 ±12	-779 ±20	10 ±30	762	769 ±49	28.1	4.2	26.7			0 ±46			573	97	
		D (lower)	1265 ±33	-2018 ±10	-739 ±38	67 ±32	634	672 ±41	28.3	4.3	27.2			69 ±47				71	
		site	1209 ±32	-2052 ±11	-843 ±36	78 ±18	737	765 ±49	28.1	4.3	27.0			51 ±18				156	

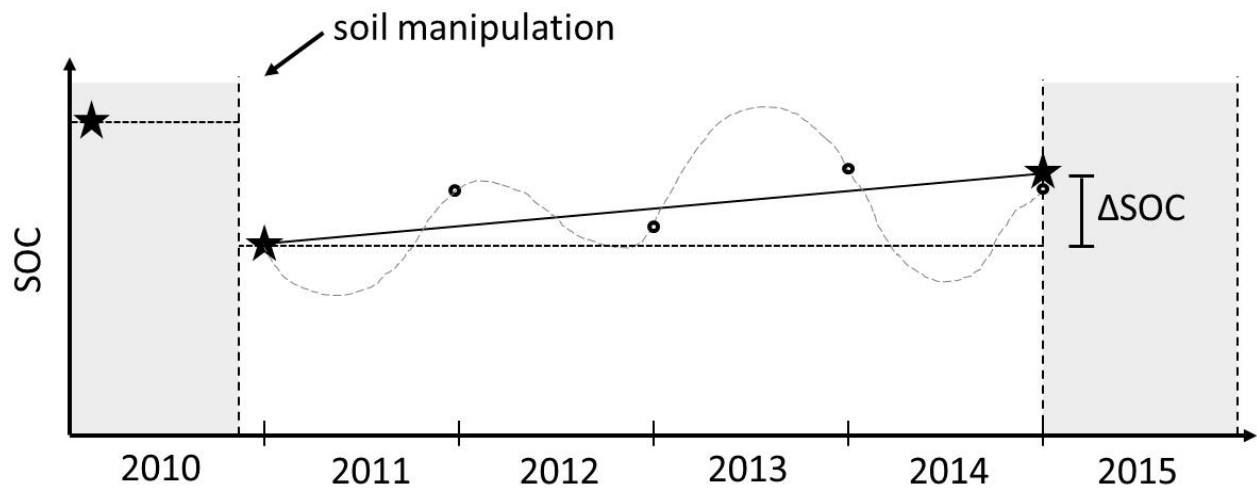
\*for comparability reasons the NECB is given using the soil sign convention (negative values = soil C loss; positive values = soil C gain)

872 \*\* NPP<sub>shoot</sub> is based on biomass samples collected next to each chamber because no chamber harvest was performed for *winter fodder rye* in 2012; superscript letter indicate non-significant differences

873 (Wilcoxon rank sum test; p-value > 0.05) between measured CO<sub>2</sub> fluxes and NPP<sub>shoot</sub>.



874 Fig. 1



875

876

877

878

879

880

881

882

883

884

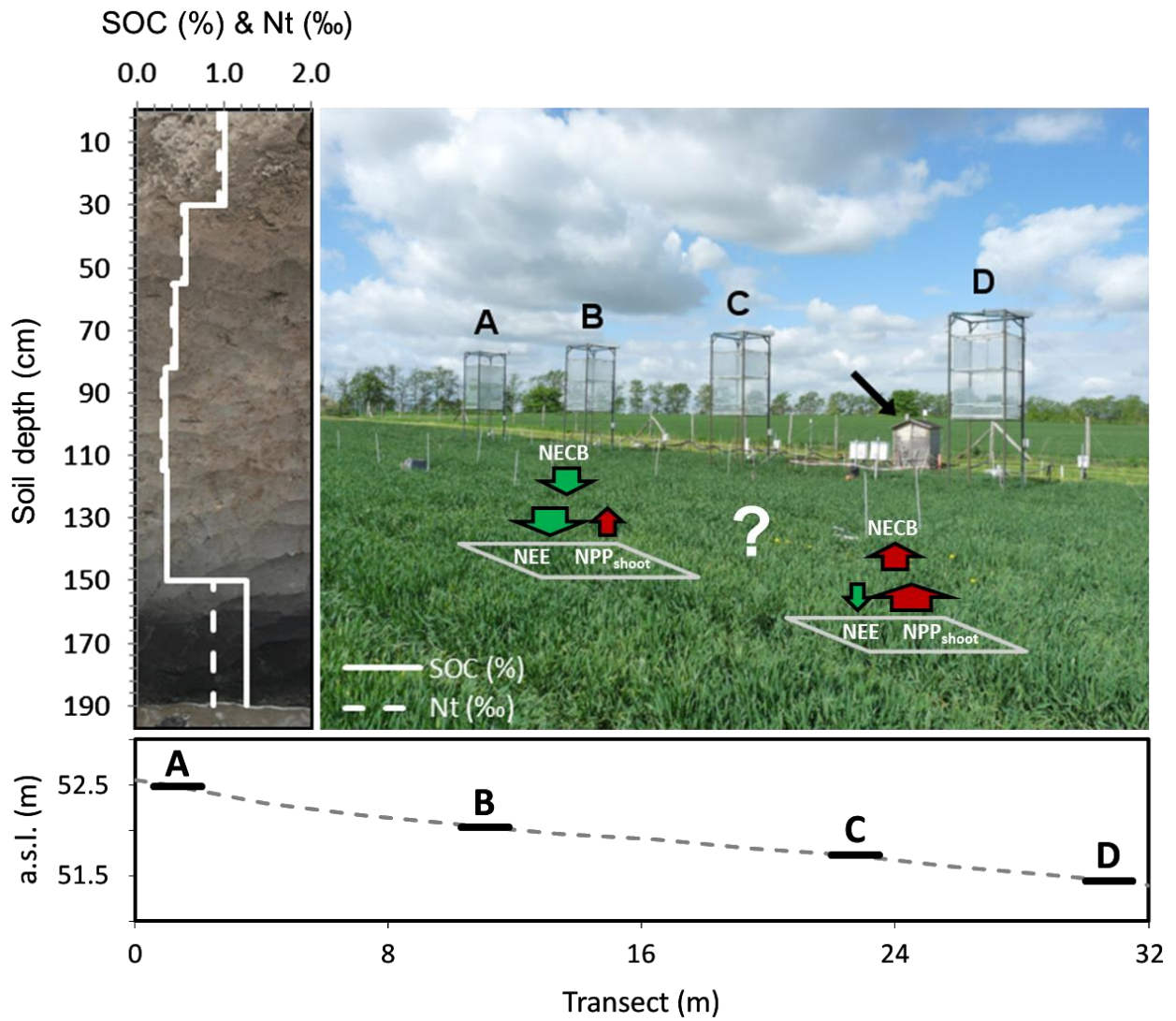
885

886

887

888

889 **Fig. 2**



890

891

892

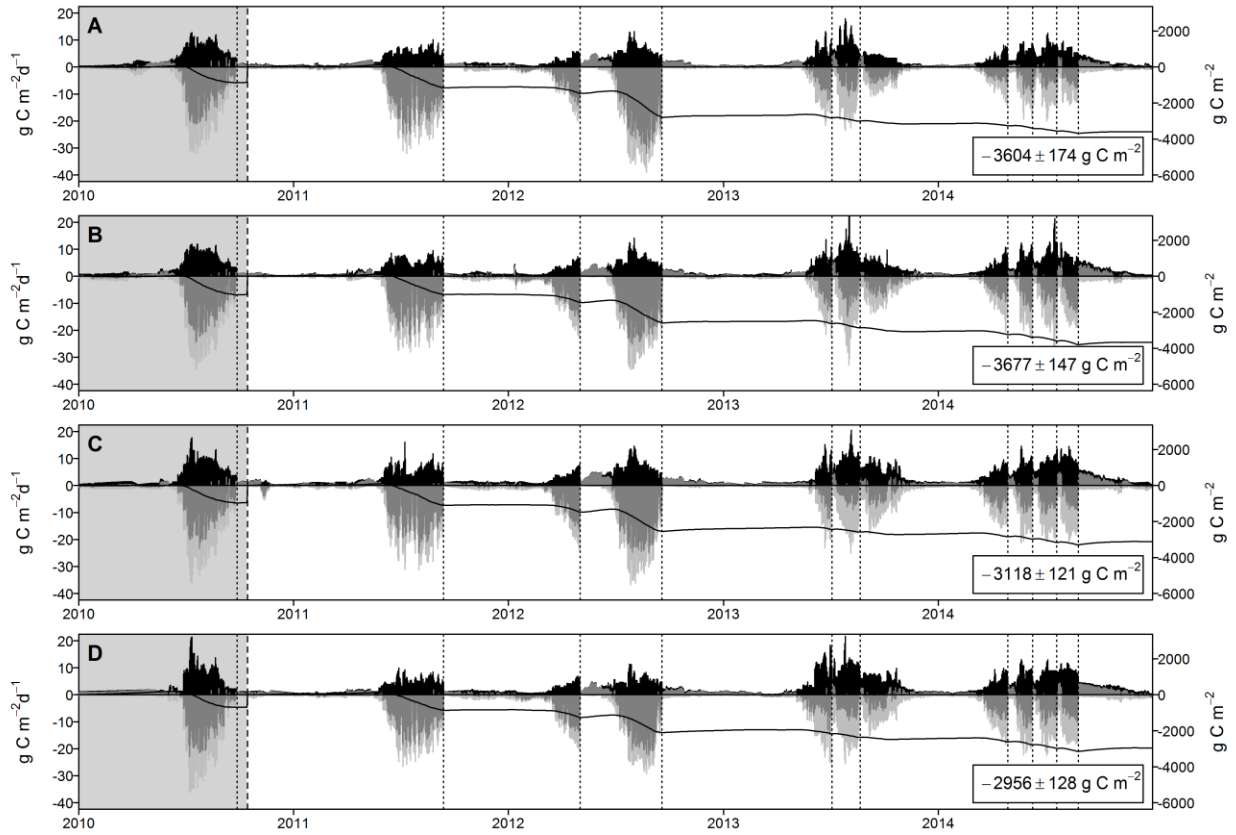
893

894

895

896

897 **Fig. 3**



898

899

900

901

902

903

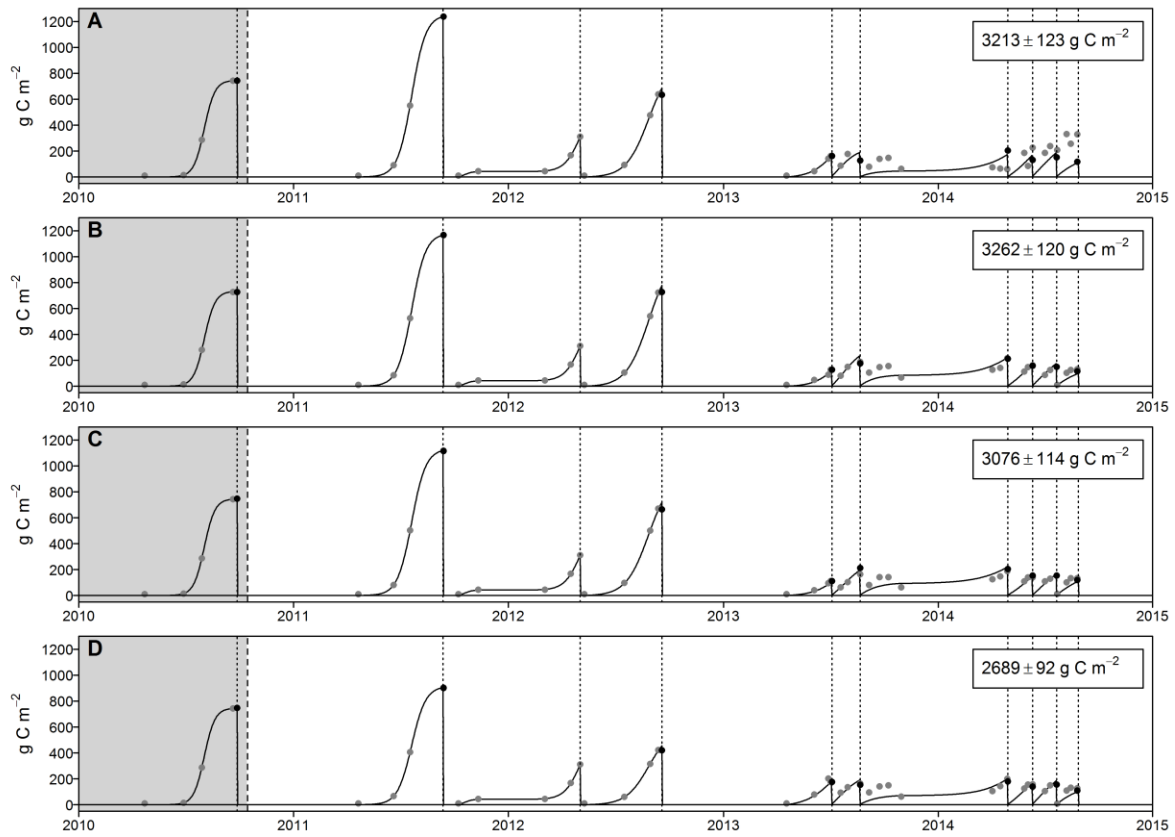
904

905

906

907

908 **Fig. 4**



909

910

911

912

913

914

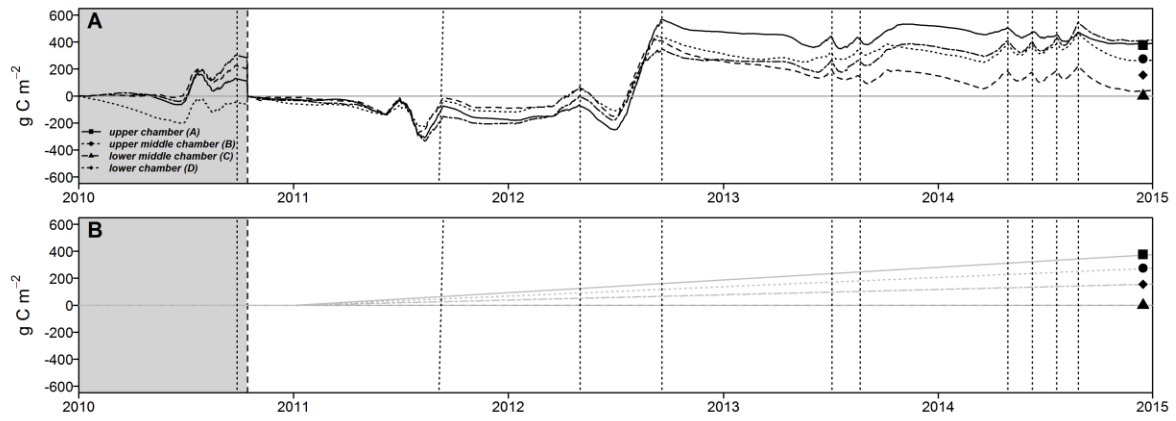
915

916

917

918

919 **Fig. 5**



920

921

922

923

924

925

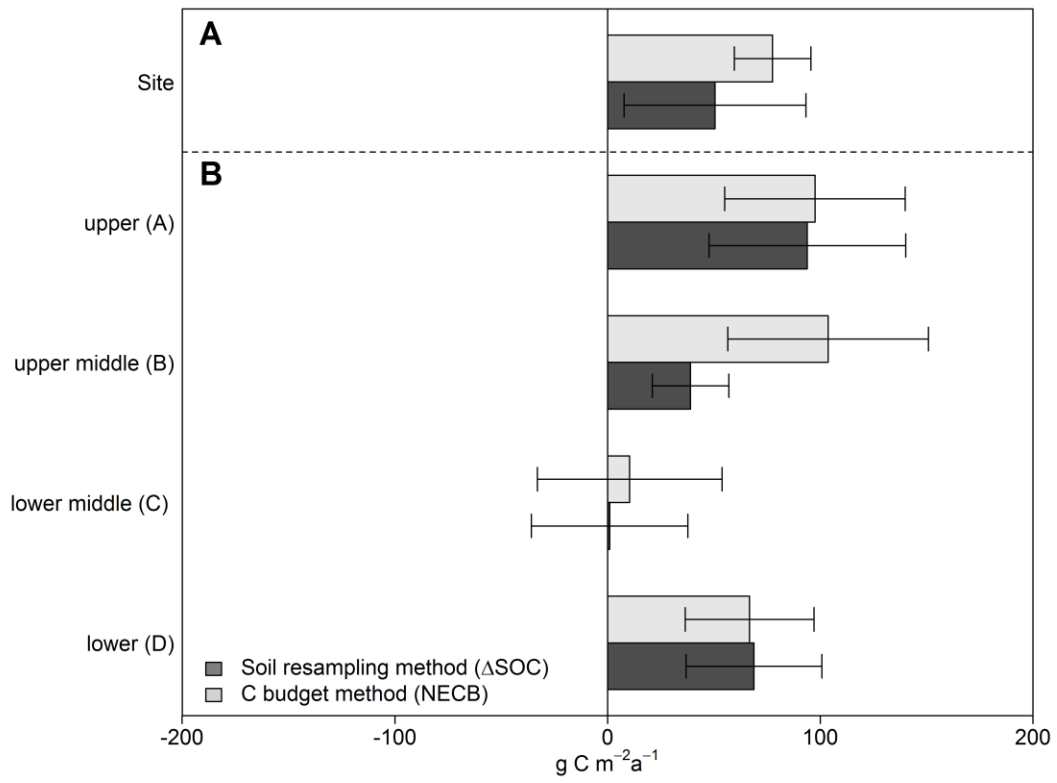
926

927

928

929

930 **Fig. 6**



931

932

933

934

935

936

937

938

939

940

941 **Appendices**942 **A.1**

Crop	Treatment	Details	Date
<b>Winter fodder rye</b> ( <i>Secale cereale</i> )	Chamber dismounting		10/04/2010
	Herbicide application	Roundup (2 l/ha)	19/04/2010
	Fertilization	KAS (160 kg/ha N), 110 kg/ha P2O5, 190 kg/ha K2O, 22 kg/ha S and 27 kg/ha MgO	23/04/2010
	Ploughing	Chisel Plough	23/04/2010
	Sowing	10 seeds/m <sup>2</sup>	23/04/2010
<b>Silage maize</b> ( <i>Zea mays</i> )	Chamber installation		04/05/2010
	Herbicide application	Zintan Platin Pack	26/05/2010
	Harvest		19/09/2010
	Chamber dismounting		20/09/2010
Bare soil	Chamber installation		27/10/2010
	Chamber dismounting		05/04/2011
	Fertilization	110 kg/ha P2O5, 190 kg/ha K2O, 22 kg/ha S and 27 kg/ha MgO	06/04/2011
	Ploughing	Chisel Plough	21/04/2011
	Sowing	10 seeds/m <sup>2</sup>	21/04/2011
<b>Silage maize</b> ( <i>Zea mays</i> )	Herbicide application	Gardo Gold Pack, 3.5 l/ha	27/04/2011
	Fertilization	KAS (160 kg/ha N)	03/05/2011
	Chamber installation		04/05/2011
	Harvest		13/09/2011
	Chamber dismounting		13/09/2011
Bare soil	Ploughing	Chisel Plough	30/09/2011
	Sowing	270 seeds/m <sup>2</sup>	30/09/2011
	Chamber installation		05/10/2011
<b>Winter fodder rye</b> ( <i>Secale cereale</i> )	Fertilization	KAS (80 kg/ha N)	06/03/2012
	Harvest		02/05/2012
	Chamber dismounting		02/05/2012
Bare soil	Ploughing		08/05/2012
	Sowing	30 seeds/m <sup>2</sup>	09/05/2012
<b>Sorghum-Sudan grass</b> ( <i>Sorghum bicolor x sudanese</i> )	Fertilization	KAS (100 kg/ha N), Kieserite (100 kg/ha), 220 kg/ha P2O5, 190 kg/ha K2O	14/05/2012
	Chamber installation		22/05/2012
	Replanting		29/05/2012
	Herbicide application	Gardo Gold Pack (3 l/ha), Buctril (1.5 l/ha)	12/07/2012
	Harvest		18/09/2012
Bare soil	Chamber dismounting		19/09/2012
	Ploughing	Chisel Plough	09/10/2012
	Sowing	400 seeds/m <sup>2</sup>	09/10/2012
<b>Winter triticale</b> ( <i>Triticosecale</i> )	Chamber installation		19/10/2012
	Chamber dismounting		20/09/2012
	Chamber installation		17/10/2012
<b>Luzerne</b> ( <i>Medicago sativa</i> )	Ploughing; fertilization	Chisel Plough; 44 kg/ha K2O, 48.4 kg/ha P40	15/04/2013
	Sowing	22 kg/ha	18/04/2013
	Harvest (first cut)		04/07/2013
	Fertilization	88 kg/ha K2O	10/07/2013
	Harvest (second cut)		21/08/2013
	Fertilization	200 kg/ha K2O, 110 kg/ha P2O5	27/02/2014
	Harvest (first cut)		29/04/2014
	Harvest (second cut)		10/06/2014
	Harvest (third cut)		21/07/2014
	Harvest (fourth cut)		27/08/2014
	Chamber dismounting		28/08/2014

944 **A.2 Weather and soil conditions**

945 A.3 shows the development of important environmental variables throughout the study period  
946 (January 2010 – December 2014). In general, weather condition were similarly warm (8.7°C) but  
947 also wetter (562 mm) compared to the long-term average (8.6°C; 485 mm). Temperature and  
948 precipitation were characterized by distinct inter- and intra-annual variability. The highest annual  
949 air temperature was measured in 2014 (9°C). The highest annual precipitation was recorded during  
950 2011 (616 mm). Lower annual mean air temperature and comparatively drier weather conditions  
951 were recorded in 2010 (7.7°C; 515 mm) and 2013 (8.5°C; 499 mm). Clear seasonal patterns were  
952 observed for air temperature. The daily mean air temperature at a height of 200 cm varied between  
953 -18.8°C in February 2012 and 26.3°C in July 2010. Rainfall was highly variable and mainly  
954 occurred during the growing season (55 % to 93 %), with pronounced heavy rain events during  
955 summer periods, exceeding 50 mm d<sup>-1</sup>. Despite a rather wet summer, only 67 mm was measured  
956 in March and April 2012, the driest spring period within the study, resulting in late germination  
957 and reduced plant growth. Annual GWL differed by up to 77 cm along the chamber transect and  
958 followed precipitation patterns. Seasonal dynamics were characterized by a lower GWL within the  
959 growing season (1.10 m) and enhanced GWL during the non-growing season (0.85 m). From a  
960 short-term perspective, GWL was closely related to single rainfall events. Hence, a GWL of 0.10  
961 m was measured immediately after a heavy rainfall event in July 2011, whereas the lowest GWL  
962 occurred during the dry spring in 2010. From August 2013 to December 2014, the GWL was too  
963 low to apply the principal of hydrostatic equilibrium; therefore, the groundwater table depth (> 235  
964 cm) had to be used as a proxy.

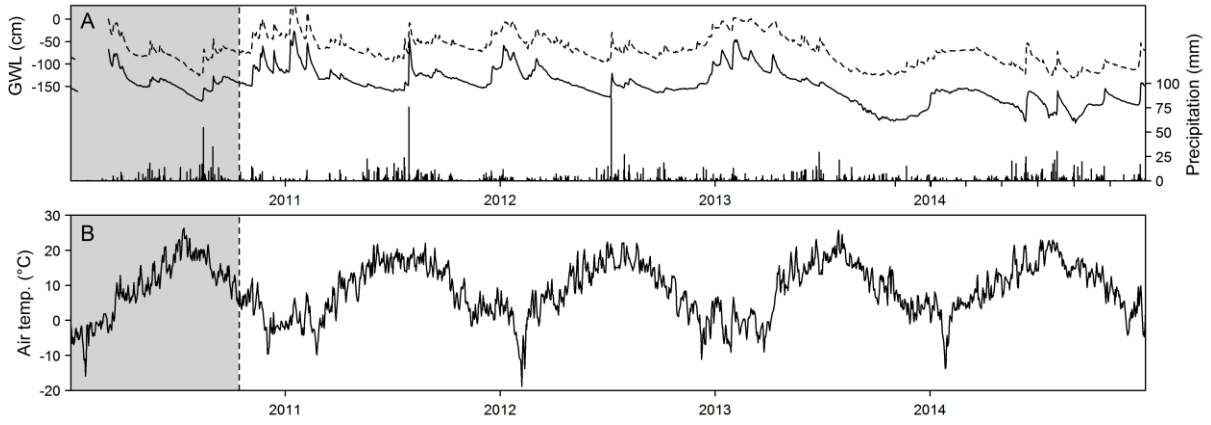
965

966

967



968 **A.3**



969

970